Revista Brasileira de Física, Vol. 15, nº 4, 1985

Theory of Glass*

N. RIVIER

Center for Nonlinear Studies, Los Alamos National Laboratory, Los Alamos, NM 87545, USA; Institute for Theoretical Physics, University of California, Santa Barbara, CA 93106, USA and (permanent address) Blackett Laboratory, Imperial College, London SW7 2BZ, Great Britain.

Recebido em 11 de outubro de 1985

Abstract The physical properties of glass are direct consequences of its non-crystalline structure. The structure is described from a topological point of view, since topology is the only geometry surviving non-crystallinity, i.e. absence of metric and trivial space group. This fact has two main consequences: the overall homogeneity of glass is a gauge symmetry, and the only extended, structurally stable constituents are odd lines (or 2π-disclinations in the elastic continuum limit). A gauge theory of glass, based on odd lines as sources of frozen-in strain, can explain those properties of glasses which are both specific to, and universal in amorphous solids: low-temperature excitations, and relaxation at high temperatures. The methods of statistical mechanics can be applied to give a minimal description of amorphous structures in statistical equilibrium. Criteria for statistical equilibrium of the structure and detailed balance are given, together with structural equations of state, which turn out to be well-known empirically among botanists and metallurgists. This review is based on lectures given in 1984 in Niteroi. It contains five parts: I - Structure, from a topological viewpoint; II - Gauge invariance; III - Tunneling modes; IV - Supercooled liquid and the glass transition; V - Statistical crystallography.

I - STRUCTURE OF GLASS FROM A TOPOLOGICAL VIEWPOINT

1.1 - Introduction

Glass spans nearly 60 centuries of human activity, from early glazed objects (4000 BC) and glassy beads which appeared in Egypt between 3200 and 2500 years BC (depending on the encyclopedia), to metallic glasses, discovered and developed in the (19) sixties and seventies. Yet, from a condensed matter physicist's point of view, it is an ill-understood material, full of fascinating and surprising physical properties.

* This is an invited review article.

The methodology of condensed matter physics consists in identifying, and relating to each other, the physical properties, structure, and constitutive elements of a class of materials. Glasses have several physical properties which are both universal and specific to disordered condensed matter (cf section 1.2), but emphasis on[1], and demonstration of (see eg.[2]) their universality have only recently been made. To relate these properties to the structural constituents requires an understanding of the structure of glass, which, at first sight, consists almost exclusively of negative statements: no metric geometry, trivial space group, no generative symmetry, no Bloch states, no single ground state, no unique best structure, etc.

By contrast, perfect crystalline materials have easily discernible structure (space group) and constituents (atoms, electrons, holes, unit cell). However, rare are the physical properties of perfect crystals which depend specifically on their space group. But *imperfect* crystals have properties directly and crucially affected by extended structural constituents, or defects (vortices, dislocations, flux lines), whose definition, label and existence (structural stability) is granted by the structure of the material[3]. We shall see that the physical properties of glasses are also governed by a single, extended constituent, the odd line or 2π-disclination[4], which is the only structural element surviving the absence of generative homogeneity and the triviality of the space group.

The main purpose of this part is to identify those universal properties and structural constituents, both at the lowest level of specificity. The level of understanding of glass is similar to that of crystalline solid state physics before 1920-30, i.e. before quanturn statistics, Bloch theorem, electron bands and dislocgtions were introduced. General concepts are required, howeveroversirnplified, rather than the solution of a particular problem from first principles. It will turn out that even such a sirnplified description yields non-trivial results.

1.2 - Universal properties of glasses

We shall list those properties which occursowidely in glasses that they can be regarded as universal, and so rarely or never in crys-

tals that they can be viewed as specific to disordered condensed matter.

a) Tunneling modes

At low temperatures, the glass is an elastic solid with overall homogeneity, capable of supporting phonons of wavelength long enough to average over any inhomogeneity. Glass can ring, as Mozart, and probably others found out long ago. Surprisingly, this is not all. At low temperatures, the specific heat is linear in temperature, and this contribution dominates the T^3 phonon contribution below 1K. The thermal conductivity is lower than that of the corresponding crystalline material (eg. quartz) and goes as T^2. The specific heat betrays the preserice of additional localized elementary excitations (1-10 per 10^6 atoms), which can absorb phonons and thereby reduce the thermal conductivity[5]. It was suggested by Anderson, Halperin and Varma, and independently by W. A. Phillips, that these additional excitations were tunneling modes between potential minima, or valleys, distributed at random in configuration space[6]. These valleys are few and far away in configuratiori space, so that tunneling occurs between pairs, thereby forming two-level systems. The main evidence for tunneling, and for a finite number of levels, comes from the fact that the ultrasonic absorption can be *saturated*. Also, echo spectroscopy can be performed, exactly as for an assembly of spins 1/2 [7].

The concept of tunneling modes has been entirely succesfuly both in explaining existing experiments, and in suggesting new ones. Tunneling modes occur in metallic and covalent glasses[2]. But, what is it that moves, let alone tunnel? How are we to label the valleys in configuration space and determine their distances? (The height of the saddle points between valleys should be of the order of the glass transition temperature). Answers in part III.

b) Viscosity, relaxation rates, entropy and the Kauzmann paradox

Traditionally, glass transition is defined to coincide with the change in the thermal expansion coefficient from a value characteristic of a liquid to that of a solid. This corresponds to a viscosity of the order of 10^{13} poises. The transition is smooth and its temperature T_g depends on the cooling rate and on the thermal history of the system.

The viscosity (or any inverse transport relaxation rate) increases smoothly and rapidly with decreasing temperature, and follows the empirical Vogel-Fulcher formula[1,105]

$$\eta = \alpha \; e^{c/(T-T_0)} \tag{1.1}$$

over a wide range of temperatures. Equation (1.1) is used by the National Bureau of Standards for calibrating references glasses[8]. The various names under which it is known in different fields (WLF, Cohen-Turnbull, Tammann, Doolittle, etc., for glasses, polymers, oils, etc.), should support its claim to universality, even though, for some glasses, finite viscosities have been measured below T_0, and the viscosity seems to cross over from (1.1) to Arrhenius behaviour as the temperature is lowered[9]. Thus, roughly, glass behaves like a supercooled fluid above T_0, and an elastic, random solid below T_0. T_0 is well above room temperature for window glass ($a\text{-}SiO_2$) whereas T_0 = 127.1K for glycerol. Slow modes in the supercooled fluid become frozen (quenched) below T_0.

A measure of the entropy of a glass is obtained by integrating under the specific heat curve, with a known value for the entropyofthe liquid as initial condition. Its value depends on the cooling rate, but, if extrapolated to zero cooling rate, the entropy becomes negligibly small at and below the *same* finite temperature T_0, at which the extrapoiated viscosity (1.1) diverges[1]. This vanishing entropy at a finite temperature is called Kauzmann's paradox, even though it was probably known to Simon. A good discussion of the meaning of entropy of glasses as measured by this method, can be found in a recent paper by Jaeckle[11].

Unlike gases, whose viscosity is proportional to the atomic diffusion rate and increases with increasing temperature, viscous or supercooled fluids have fluidity $1/\eta$ - ability to yield to a shearing stress - proportional to the mobility of a diffusing object or "defect", i.e. to its diffusion rate D, by Einstein's relation. One would expect D to be activated in condensed matter, and $1/\eta$ to decrease with decreasing temperature as in eq. (1.1), but with $T_0 = 0$ [12]. The other problem is: which "defect"? Answers in IV.

c) Energy gap

Window glass is transparent, and amorphous semiconductors have

a gap. Despite the absence of long-range order and of Bragg reflection, the existence of a gap was shown by Weaire[13] to be a consequence of the fixed valence in amorphous semiconductors, i.e. to the uniformity in vertex coordination z, or regularity of the graph describing their structure (cf section 1.3). Furthermore, for a simple but realistic model, Weaire and Thorpe[14] have shown that the energy spectrum consists of degenerate states and of the spectrum of eigenvalues of the connectivity, or adjacency matrix (a matrix describing the topology of the graph). The gap is filled by localized defects (eg. dangling bonds) and modified by many-body effects (polarons, excitons). The subject is treated in M.H.Cohen's work in ref. 106,

d) Hall effect

The Hall effect is doubly anomalous in amorphous semiconductors: "...two orders of magnitude less than expected.. ., almost invariably it has the wrong sign"[15]. The magnitude of the effect suggests interferenceof the electron wave packet, dueto the fact that the space in which it propagates is not simply connected. The cores of line "defects" puncture the space available to the charge carriers.

1.3 - Structure

See references 16 and 17 for details.

Glasses belong to either of two classes: covalent glasses (like window glasses or *a-Si*) or random packings (like metallic glasses). In both cases, their structure can be described by a *regular graph.*

In covalent glasses (Pl.1), vertices and edges of the graph are atoms and bonds, respectively, (non-planar) faces are rings, and cells do not have a direct physical interpretation. The atoms have fixed valency, so that the graph has fixed vertex coordination z (z=4 for Si), and is said to be *regular.* Dangling bonds are permitted. This graph is also called a *continuous random network* (CRN).

In metallic glasses, only vertices have direct physical interpretation (atoms), and neighbourhood (edges) must be defined precisely. This is done by *Voronoi construction,* a partition ofspace whereby any point belongs to the territory of the nearest atom. Every atom is

Pl.l-Continuouç random network, exhibiting homogeneity, non-collinearity and odd lines (the ribbons, which thread through odd rings exclusively).

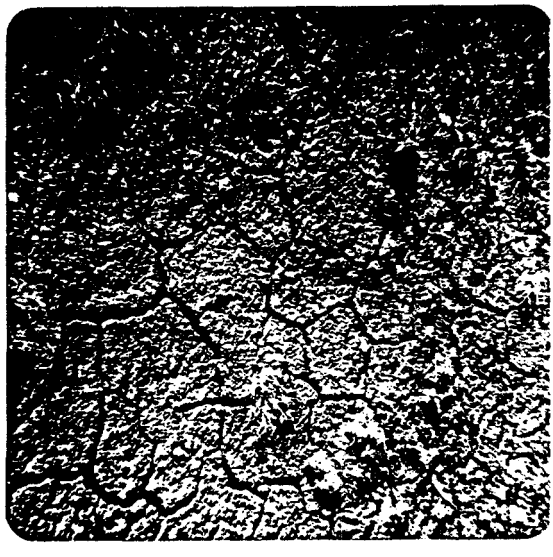

Pl.2 - Mud cracking.

thus ascribed a (convex) polyhedron or cell, and the packing is a space-filling assembly of such cells. The assembly of Voronoi polyhedra, with their (planar) faces, (straight) edges, and vertices, form a graph, called *Voronoi froth*, which is regular (z=4 in 3D and z=3 in 2D) because any vertex with higher coordination can be split into several regular vertices by an infinitesimal deformation of the packing (through transformation T1 of section 1.5). They are not topologically or structurally stable, and occur with negligible probability. Thus the Four Corners boundary between Colorado, Utah, Arizona and New-Mexico, is a cartographer's conspiracy and is not geographically stable. Similarly, in 3D, only edges where 3 faces or cells meet are structurally stable. Structural stability is what Lewis[21] calls "random avoidance of the niceties of adjustment", and the structural elements (vertices, edges, etc.) are simply territorial boundaries of a random packing. By contrast:, CRN (covalent glasses) have vertex coordination given by chemical, not territorial considerations, and more than 3 (non-planar) faces can meet on a single edge, even though their vertices are still - in SiO_2 or a-Si - all tetra-coordinated. The crystalline analogues to the Voronoi construction are the Wigner-Seitz cells, or, in reciprocal space, the Brillouin zones.

Let us return to the original packing. Each atom corresponds to a Voronoi polyhedron or cell. Two atoms are neighbours, and will be joined by an edge, if their Voronoi polyhedra share a face. Thus, two graphs, related by *duality*, describe the same packing, the original atomic packing, and the Voronoi froth. Only the Voronoi froth is regular. The packing has high, fluctuating vertex coordination ($\langle z^* \rangle \approx 13.4$, increasing with anisotropy of the Voronoi polyhedra, and decreasing if the polyhedra have different volumes[18], as happens in real mettalic glasses made of at least two different elements). The self-dual condition is $z = z^* = 6$ in 3D and 4 in 2D (cubic and square lattices, respectively).

The essential feature is the considerable variety of shapes of Voronoi polyhedra. Matzke[19] has identified 100 different kinds in soap bubble froth, out of which 20 occur frequently. Thus, there is no single unit cell in glasses, not even smooth deformations thereof. The 20 Voronoi polyhedra are all topologically different, and the structure of one metallic glass is a member of a statistical ensemble (of most prob-

able distributions - see part V). Moreover, glasses belong to a different class of packings than the aperiodic tilings of Robinson and Penrose, which have only a few elementary geometric tiles[20]. The situation has been summarized in 1943 by the botanist F.T. Lewis: "The average 14-hedral shape observed in massed bodies of diverse surface tension may be due to random avoidance of the niceties of adjustment. Failure to arrange the bodies so that 5 or 6 meet at a mathematical point, or form intersection where 4 meet along a mathematical line is sufficient to account for *promiscuous, unoriented polyhedra* having an average of 14 facets"[21]. This failure, associated with structural stability, gives rise to a substantial variety of cell shapes, and to statistical equilibrium.

Voronoi froths and continuous random networks are topologically equivalent: they have the same, low vertex coordination $z=4$, but CRN's have bent edges, nonplanar faces, nonconvex cells and two faces sharing more than one common edge, whereas Voronoi froths have straight edges, planar faces, convex cells, but unequal edge lengths. The ring statistics is accordingly different: Voronoi froths have a majority of 5--bond rings, CRN's 7-bond rings[22].

The Voronoi partition of space can be extended to packings of different atoms (as befits real metallic glasses) and unequal cells. This is not as elementary as its sounds: Consider 3 atoms in 2D; they form the vertices of a triangle, whose perpendicular bissectors are concurrent, by an elementary theorem of geometry. If the atoms are unequal, which perpendicular division retains concurrence, and thus space-filling? There is only one known answer, the *radica2 axis*, a straight line (a plane in 3D) wich is the locus of points with equal tangents to two circles (spheres) representing the atoms. It is obvious that radical axes are concurrent, less so that they are straight lines, and the proof of this last statement[2'] (an elegant exercise in inversion geometry) strongly suggests that the radical froth is the only generalization of the Voronoi froth to unequal atoms. It has been applied to metallic glasses by Gellatly and Finney[24].

The Voronoi construction has been used to describe not only glasses, but also ecological and geographical problems, soap bubbles froths, metallurgical aggregates, convective cells, etc.[17].

1.4 - The need for topology and its consequences

Manifestly, amorphous structures have neither global length scale (ruler), nor unique global reference frame orientation (compass). In fact, amorphous or non-crystalline materials are characterized, at first sight, by what they are or have not: No generative symmetry (translation or rotation), *trivial* space- or point groups, *no* unique ground state (see tunneling modes), no Bloch theorem,. .., so that *non*-negative concepts are required, which are structurally stable under those transformations which keep the structure unchanged.

At a glance, one distinguishes the three main structural features, not only of glasses, but of all large, space-filling random structures (metallurgical aggregates, undifferentiated biological tissues, geological jointings, etc.) :

i) Non-collinearity of local reference frames (or variety of cell shapes).

ii) Overall, but non-generative homogeneity.

iii) Odd lines.

These three features are characteristic of the amorphous state, and can be taken as its structural definition. If either (i) or (iii) are missing, one may still have a random structure, but without *topological* disorder.

Homogeneity implies that atoms are distinct, but not physically distinguishable. Glasses share this property with crystals. However, unlike in crystals, this homogeneity is not a generative symmetry, but only the fact that any objective (physical) statement (one whicti does not contain "I", "this", "here",...) about one particular atom can equally well be made about any other, even though their local environment (tetrapods attached to the Si atoms in a-Si or vitreous silica, Voronoi cells in metallic glasses) are manifestly different and non-collinear. (See Pl.1).

A CRN construction can be continued *ad infinitum*. This is the kind of homogeneity experienced by getting lost in a forest, with trees taking the part of atoms. This homogeneity of glasses rnanifests itself at a microscopic level, to the surprise of early X-ray crystallographers: "...one of the most interesting discoveries made in the comparatively early history of X-ray analysis was the fact that silk and even paper

are more crystalline than glass." (Dame Kathleen Lonsdale, quoted in ref. [25], p.26). Thus the scale of homogeneity in glass is 3 orders of magnitude smaller than the smallest microcrystallites (10 versus 1000 atomic distances).

The automorphisms probing homogeneity are permutations of the atoms (or the trees) and their surroundings, effected, for example, by *local* rotations of the tetrapods. The physical properties must be unchanged under these local transformations, and homogeneity of glasses is a genuine, *gauge* symmetry. We shall discuss gauge invariance indetail in part II. At the structural level, the most elementary such automorphisms are automorphisms of the graph, that is, permutations of the vertices which preserve adjacency. At a dynamical level, local rotations must also be included.

In the absence of a global metric and reference frame orientation, the only invariant under automorphisms probing the homogeneity of amorphous structure is their connectivity or the spatial relationship imparted by, eg., Voronoi construction. (We shall see in part V that some transformations can switch neighbours (T1), but still leave the statistical properties of the structure invariant). Thus, the relevant geometry for amorphous condensed matter is topology (rubber geometry), which replaces metric geometry of classical crystallography. By the same token, the 230 metric space groups are replaced by homotopy groups which describe connectivity. k states and Bloch theorem give way to topological sectors and to a theorem, also formulated by Bloch for superconductors[26], stating that the free energy is a periodic function of the flux triggering the gauge transformation. The period corresponds to a large, or non-trivial gauge transformation, which brings the system from one topological sector to another. The best illustration of topological invariance is given in a cartoon by Denis Weaire (Fig.1).

Consequences of this enforced retreat from metric to topology are that

a) One cannot distinguish structural constituents by their sizes alone.

b) The existence, and the definition of a structural constituent depends on its structural stability, so that it cannot be made to disappear by small, continuous deformations.

c) Its only distinctive feature is its shape. Hence randomness and topological disorder *imply* that cells have many different shapes, like

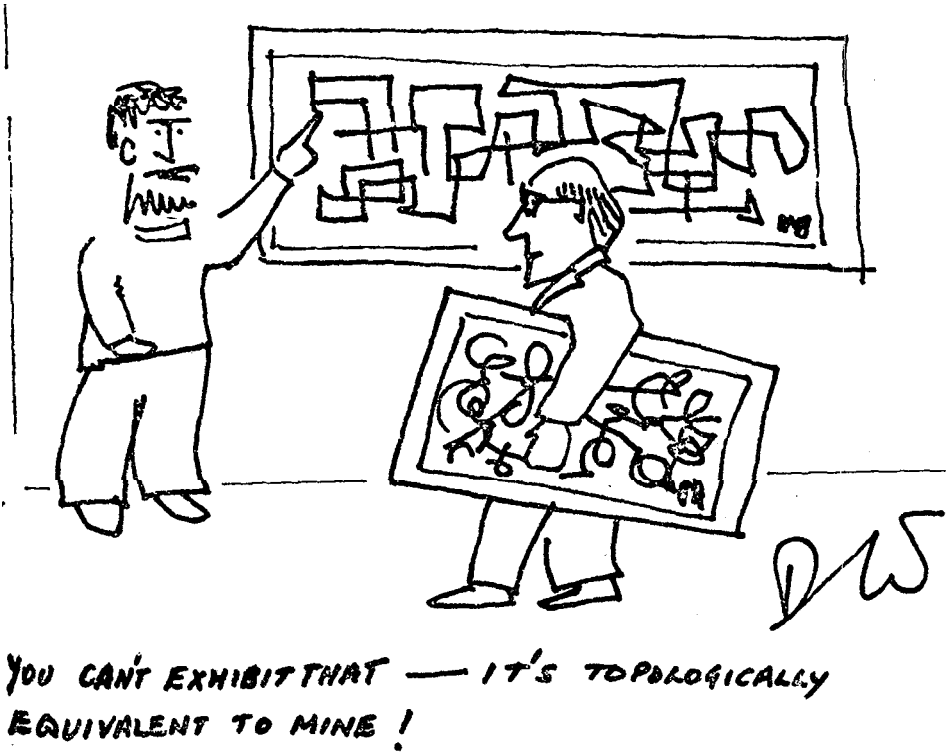

Fig.1 - Topological invariance and transformation, illustrated by Denis Weaire (based on a real event).

the various soap bubles identified by Matzke[19]. Glasses cannot be made of only one type of cell, as a result of "random avoidance of the niceties of adjustment" [21]. The problem of the structure isa statistical one, and the methods of statistical mechanics yield the average features (its "equation of state", which is called Lewis's law in the case of cellular structures, see refs. [27], [57], or part V) of the ideal random, space-filling structure (the class of most probable members of an *ensemble* of structures). This equation of state is a correlation betweensizesandshapesof theconstituting cells, and implies a medium-range correlation (one should not say order) in the amorphous structure.

1.5 - Elementary structural transformations

There are three, local, elementary transformations of a random structure under small, continuous deformations[17,28].

i) T1, or neighbour-switching. (Fig.2).

ii) T2, or cell disappearance. (Fig.3).

ii') Mitosis, or cell division. (Fig.4).

All of which occur in 2D and in 3D. In addition, in 3D, one has

iii) Face disappearance.

All these processes (or their inverse) occur in froths, foams or emulsions, in rock or mud cracking, and in convection cells. Voronoi froths have a conserved number of cells, and do not accomodate (ii) or (ii'). Covalent networks (CRN) only have T1 transformations, which is there a local valence or bond exchange. (The term "valence alternation" is now used to describe a particular class of non-local transformations, accompanied by charge transfer and change in vertex coordination, which control the electronic and optical properties of amorphous chalcogenides[28]). The T1 or neighbour-switching process is also that which restricts topological stability to 3- (in 2D) and 4-coordinated vertices (in 3D), only. Note that it conserves the vertex coordination of the froth, but not that of the dual graph. In this respect, it affects adjacency, but we shall see in part 5 that the statistical properties of the structure remain invariant.

There have been several recent attempts to construct random networks by applying successive, random T1 transformations on an initially regular (hexagonal or diamond) lattice in 2D [29,30] or 3D [31]

These transformations change the number of edges of the faces involved. In 2D, this corresponds to the introducing of topological disclinations (rotation dislocations). Hexagons tile the plane (or the floor of a kitchen). Removing or adding one edge to one hexagon can be done by making a cut in the tiling, removing or adding a wedge (segment) of material and reglueing. One recovers a perfect hexagonal tiling apart from the cell at the end of the cut which is now pentagonal or heptagonal, and the fact that the tiling is now warped. It has positive, or negative curvature. The non-hexagonal cell is a disclination, and imparts curvature, through the Gauss-Bonnet theorem of geometry. 12 pentagonal cells transform your kitchen floor into a football, an elemen-

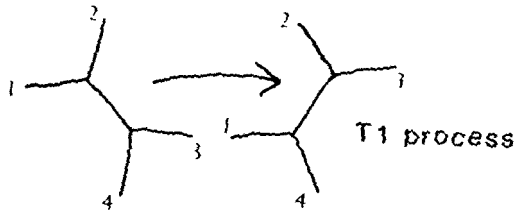

Fig.2 - Elementary local rearrangement of cells.

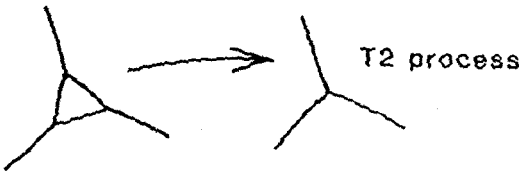

Fig.3 - Vanishing of a cell.

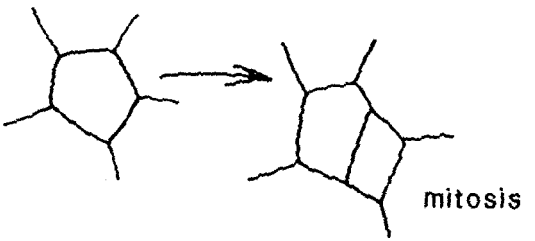

Fig. 4 - Cell division.

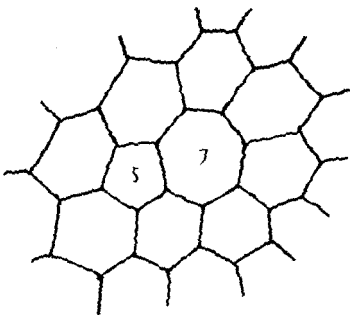

Fig.5 - A 5-7 pair of cells, making up a topological dislocation in an othetwise hexagonal structure.

tary consequence of Euler's theorem to be discussed in the next Section.

This geometrical picture no longer holds completely in 3D, where there is no Gauss-Bonnet theorem. In relaxed networks or froths, faces have on average 5.1 edges (Voronoi froth[18]) or ≈ 7 edges (CRN[22]) so that there is no unique regular, flat packing. More to the point, disclinations exist, and are labelled in amorphous materials whose space group is trivial, by the fundamental group of rotations[3,4] $\pi_1(SO_D)$. In D = 2, $\pi_1(SO_2) = Z$, and disclinations, labelled by sign and intensity, exist, whereas $\pi_1(SO_D) = Z_2$ for $D \geq 3$, and the only topologically stable line "defects" are odd lines (see below). Nevertheless, even in 3D, curvature associated with the number of edges per face remains an useful concept to describe the *local* strain.

A dipole of neighbouring 5- and 7-sided facesformsadislocation (Fig.5). (Again, this is only a local concept in 3D, without topological stability). The dislocation has the following physical properties in *random* networks:

1) It can glide (by using T1 transformations). This determines the elastic and plastic properties of commercial foams[32]. It also constitutes a very efficient way of dissipating shear energy. This property finds an amusing illustration in the structure of daisies, pinecones or pineapples (phyllotaxis)[33].

2) It can climb. A mitosis (or a T1 transformation) creates a pair of dislocations, and subsequent mitoses of the larger cells, corresponding to a glide of the two dislocations away from each other, leaving an additional layer of cells in between (Fig.6). Again, as far as elastic energy is concerned, this is a very efficient method of solving the problem of coping with additional material (growth of biological tissues[34] or of metallurgical grains[35]). Hillert's mechanism is slightly more complicated as it involves creation of 3-sided cells (in 2D) only (a combination of T1 and T2 transformations, exclusively).

Morral and Ashby[36] have given a very clear representation of these transformations and defects in 3D ordered foams or grains packings. In particular, the dislocation core forms one *single* odd line (cf. fig. 11a of ref. [36]), which shows that topological concepts applicable in 2D cannot always be transposed *verbatim* to 3D. The glide of the dislocation occurs through succesive T1transformations, as in 2D. It is

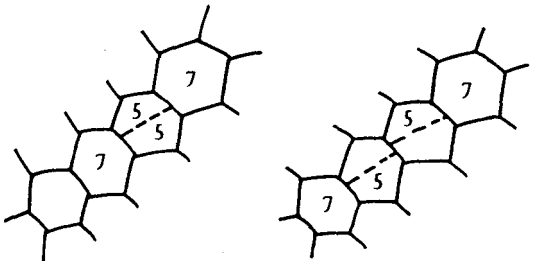

Fig.6 - Creation and dissociation of a dislocation pair by successive cell divisions.

emphasized that all these are *local* transformations, which do not require long-ranged mass transport, unlike dislocation climb in crystals.

3) Dislocations screen the strain due to disclinations (curvature). For example, structurally, a radiolaria (microscopic marine animal) is a large football, and uses dislocations to screen the strain from the 12 disclination required by topology (football = sphere). The same screening of (topologically stable) disclinations by dislocations (which are not topologically stable in glasses) occur in an elastic continuum representation of glass[40,57].

4) Dislocations enable disclinations to move. (For example, a T1 transformation next to a disclination creates a dislocation and moves the disclination).

All these properties emphasize the *dynamical* role of dislocations, which is particularly effective in random structures, where dislocations are not topologically stable, and can be regarded as local strain fluctuations fulfilling a specific, physical purpose.

Although these transformations have been introduced here from a purely mechanical point of view, one can show (part V) that they also leave the statistical properties of the random structure (average shapes and their correlations) invariant, so that they can occur independently of each other, anywhere in space or time, without affecting the statistical equilibrium of the structure. They play the same part in statistical crystallography that *microreversibility* plays in statistical thermodynamics.

1.6 - Topological conservation laws in random structures

Topologically stable constituents of disordered condensed matter are those which retain their identity (and their existence) under small, continuous deformations of the system (including its motion). For example, a dislocation in a crystal is topologically stable, an arbitrary elastic distortion, usually not. Topological stability can be expressed as a conservation law or a continuity equation. In random networks or froths, there are two conservation laws:

1) Euler's relation

$$F - E + V = \chi \qquad (2D)$$

$$-C + F - E + V = 0 \qquad (3D) \qquad (1.2)$$

for a space-filling graph with V vertices, E edges, F faces and C cells (including the cell at ∞). The Euler-Poincaré characteristic χ is a topological invariant of the manifold (space) containing the network or the froth. It is an integer of order 1 ($\ll$ V, E, F in systems with a large number of elements). Euler's relation is easily proven by induction, adding elements to a given network. In particular, one can verify that the left-hand sides of equations (1.2) are invariant under the elementary transformations of section 1.5. Indeed, their physical properties set the time scale for topological evolution, which is much longer than that of non-topological deformations (the latter, typically of order a/c, where a is the average spacing between atoms and c, the speed of sound).

2) Odd lines

The second conservation law is even simpler, and applies to 3D structures: The presence of five- or seven-sided faces in a structure is symptomatic of its non-crystallinity, being incompatible with simultaneous rotation and translation symmetries. Odd-membered rings (faces with an odd number of edges) are not found in isolation, but are threaded through by uninterrupted lines, which form closed loops or terminate on the surface of the material[4] (cf. the ribbons of Pl.1).

Thus, odd faces are not isolated elements, but linear objects which are topologically stable. They are claracterized by oddness,

rather than intensity. However, because these objects are lines, they remain difficult to eliminate despite their modulo *2* algebra.

There are two, similar proofs of this conservation law. Both rely on the construction of an *arbitrary,* closed surface S, homeomorphic to a sphere for simplicity, which intersects the random network at its vertices. S contains therefore some vertices, edges and faces of the network, which triangulate S (this can always be arranged by small deformation of S). The assertion is proven if, for *any* S, there is an even number of odd faces on S (providing an exit for any odd line entering S).

i) Ascribe a weight $J_e = (-1)$ to every edge e on S, arid an index $\Phi_f = \prod_{e \in f} J_e = \pm 1$ (even/odd face), to every, face f on S. Then, $\prod_{f \in S} \Phi_f = \prod_{e \in S} J_e^2 = 1$ (J_e enters twice in the product because every edge belongs to 2 faces on S). q.e.d.[37].

ii) Let e, f_i denote the number of edges, i-sided faces on S The incidence relation between edges and faces, $2e = \Sigma i f_i$, impliesthat $\sum_{i \text{ odd}} i f_i = even$, and, because $i f_i$ and f_i have the same parity for i odd, $\sum_{i \text{ odd}} f_i = even$. q.e.d. [4].

The second proof suggests a generalization of the odd line conservation law to 2D surfaces of arbitrary Euler-Poincaré characteristics and networks of constant vertex coordination[38], and also to the structure of polyhedral networks (a model of amorphous packings with tetrahedra and octohedra of atoms as elements, proposed by Ninomiya[39] to describe medium-range "order" in amorphous packings).

For some amorphous materials, like polymer glasses, it may be too difficult or complicated to construct a random network describing the structure. The simplest, and least specific description of any glass is as an *elastic continuum,* with a trivial space group (ie. without any infinitesimal translational and rotational symmetries). (A crystal can also be represented as an elastic continuum, but with either full (Volterra continuum), or discrete (one of the 230 space groups) symmetry). Odd line is the *only* stable structural constituent surviving the transition from discrete, cellular network, to continuum. (Cells,..., ie. simplices have disapeared). It takes then the form of 2π-disclination. This can be shown very simply[40]: Consider a configur-

ation at a point, and take it for a walk in space, while maintaining its orientation relative to the local reference frames (parallel transport) (Fig.7). Upon returning to the starting point, the configuration, which determines the physical properties (strain, etc.) of the system, must either be restored to its original orientation, or any mismatch must be physically irrelevant. The latter situation applies tocrystals, where possible mismatches are elements of the space group, which label the Burgers vectors of dislocations and disclinations. In glasses, the space group is trivial and the configuration must be restored to its original orientation. Nevertheless, there are still *two* possible transformations of the local configuration upon circumnavigation: a rotation by 4π is homotopic (continuously deformable) to the identity, but rotation by 2π entangles connection of the local configuration with the rest of the system. Thus, one remains with one single structurally stable constituent in continuous amorphous, condensed matter, the 2π-disclination which has the same algebra as odd lines in networks. Both have cores puncturing space (there is no way of filling and odd ring because the relationship between any two vertices depends on the path chosen around the ring - zero is an even number), and both are sources of non-collinearity (see P1.l). They are therefore the same specific and universal constituents of glasses which we were seeking. They are also the only ones: translations are homotopically trivial, so that dislocations of any kind are not structurally stable. Neither are point defects.

In summary:

Group of all possible local transformations (excitations) $G = T_3 \text{ A } SO_3$

Space group H = 1 A 1 (trivial)

Topologically stable constituents (labelled by non-trivial homotopy groups of G/H)[3]:

Odd lines - ..... $\pi_1(SO_3) = Z_2$

Non-singular textures -.... $\pi_3(SO_3) = Z$ (yet to be identified)

Odd lines are therefore what count as configurations in the glass (eg. in the residual entropy[41,11]), and also as slow modes in a viscous liquid or in the glass above T_0. Indeed, as long as the time scale for topological transformations is longer than that for non-topological deformations ($\approx a/c$), the flow of topologically stable objects

is a slow- or hydrodynamic mode, and any time-independant conservation law has a time-dependant correspondant. Such conservation laws are identities expressing topological stability, called *Bianchi identities.* [In electromagnetism, the first couple of Maxwell equations include a time-independant (div $B = 0$) and a time-dependant ($\partial_t B + \text{curl } B = 0$) conservation laws for the density B of topological objects. In elasticity, the topological objects are disclinations in general (dislocations in crystals, where disclinations cost a prohibitively high strain energy, and are excluded by an *ad hoc* hypothesis (distant parallelism)), and inclusion of time-dependance constitutes the standard, phenomenological generalization of elasticity to rheology and viscoelasticity[43].]

Thus, Bianchi identity plays two parts. It grants the object its topological stability. But also, it is a topological conservation law which constraints the motion of the object and of the fluid containing it.

Note that disclinations also appear in Kléman and Sadoc[44] description of the structure of glasses, as perfect crystals in an "ideal" (in the sense of Plato), *curved* space, which are projected into our usual, Euclidean space (the cave). Overall homogeneity is guaranteed by construction in the curved space, as is the best local packing (tetrahedral or icosahedral, and therefore incompatible with Euclidean space-filling requirements), and disclinations lines appear as a result of the projection[45]. Wnereas this approach and ours agree in 2D, the disclinations of Kléman and Sadoc conserve a sign and intensity in 3D, and are prevented to cut across each other by topological obstruction (they are labelled by a non-abelian group). Consequently, glass above T_0 and supercooled liquid cannot be described by the same curved space model (where flow would be akin to solving the Rubik cube), unless the tetrahedron SiO_4 (in covalent glasses), or the icosahedral cluster (in metallic glasses) order parameters, vanish at T_0.

J.C. Phillips has proposed a cluster model for chalcogenide and oxide glasses[b6]. The size of the cluster (radius $\approx$ 30 Å) fits with homogeneity discussed in section 1.4, but its surface represents a wall-like defect, which is not topologically stable ($\pi_0(SO_3) = 1$). It can be healed into line defects, as demonstrated explicitely

in the case of metallic clusters by Sadoc and Mosseri[47,45], and also in actual crystalline phases like W_β, Cu_2Mg, Mn_α, U_β [48]. This lack of topological stability does not mean, of course, that local strains are not concentrated on internal surfaces in glasses, and several experimental properties are best explained by Phillips's model. Our topological point of view analyzes glasses at a lower level of sophistication. Even then, the odd lines, which are the only ingredients at that level, are not physically irrelevant but can account for non-trivial, specific and universal properties of glasses.

II – GAUGE INVARIANCE

2.1 - Discrete gauge invariance in spin glasses

Gauge invariance in disordered condensed matter was first mentioned in a paper by Toulouse[49] dealing with spin glass on a lattice, described by the Edwards-Anderson Hamiltonian,

$$H = \sum_{(ij)} J_{ij} S_i S_j \qquad (2.1)$$

where $S_i = \pm 1$ (Ising spins on lattice points i), and the coupling between nearest neighbour spins is $J_{ij} = \pm J$, according to some probability distribution given a *priori*. Hamiltonian (2.1), and thus the physics of the system, are invariant under the *local* transformation

$$S_i' = \tau_i S_i \quad , \quad J_{ij}' = \tau_i J_{ij} \tau_j \qquad (2.2)$$

parametrized by $\tau_i = \pm 1$ (Z_2 gauge transformation). This is a local transformation, involving variables which live on vertices (dynamical variables) and on edges (connections): it is therefore a gauge transformation. Transformation (2.2) is exact. It is also not very useful, since it involves two variables of physically different status: The spins S_i are dynamical variables, allowed to reach thermodynamic equilibrium within a canonical ensemble (Boltzmann distribution). By contrast, the couplings J_{ij} are fixed (quenched) when sample under investigation was made. They are only random in the ensemble of different, but physically equivalent, realizations of similar spin glasses. It is the free energy of every particular spin glass realization which is

averaged over the couplings. In short, half of the gauge transformation $J \to J'$ is not physically realizable on a given sample.

Invariants under transformation (2.2) include not only the Hamiltonian, but also the face (or plaquette) index $\Phi = \prod_{e \in f} J_e$, and therefore the frustration (or oddness in the language of part I) $sig\ \Phi = -1$. (It is easy to show that frustration forms closed loops or lines terminating on the surface of the material, using, eg., theproof (i) of the theorem of section 1.6). Frustration is a geometrical property, independant of the "matter" field S_i, so that geometry (and essential, topological disorder) is preserved under gauge transformation. Moreover, the partition function for a *given* sample, $Z[\{J\}]$, arid thus its physics, is independant of all the details of the distribution of couplings $\{J\}$ apart from those which are gauge invariant[50]:

$$Z[\{J'\}] = Z[\{J\}] \ . \qquad (2.3)$$

In other words, the tiling (warping, curvature, oddness, ...) $\{\Phi\}$ completely characterizes the geometry of the system, and is gauge invariant. As a corollary, the unfrustrated or Mattis model ($J_{ij} = J_i J_j$ so that all $sig\ \Phi = 1$) has the same statistical mechanics as a ferromagnet.

[It is amusing to see what happens to gauge invariance within the replica formalism[51]. For simplicity, consider the infinite range model for N spins[52] with gaussian distribution of couplings. Then,

$$\langle \ln Z \rangle \to \langle Z^n \rangle = \sum_{S_i^\alpha} \exp\left[\beta^2 J^2/(2N) \sum_{ij} \sum_{\alpha\beta} S_i^\alpha S_j^\alpha S_i^\beta S_j^\beta\right]$$

which is invariant under two types of transformations: Either a local spin flip $S_i^{\alpha\prime} = \tau_i S_i^\alpha$ in all replicas, or a global rotation of each replica independently, $S^{\alpha\prime} = R(\vec{\theta}_\alpha) S^\alpha$. The Edwards-Anderson order parameter $q_{\alpha\beta} = \langle S^\alpha S^\beta \rangle$ is *not* invariant under the latter transformation, which expresses the fact that the symmetry between replicas is broken ($\langle q_{\alpha\beta} \rangle \neq 0$). The system is trapped in one of the many valleys (replicas) in configuration space, and hydrodynamic modes are associated with this broken symmetry[53,54].]

Transformation (2.2) cannot meaningfully be generalized to continuous (XY or Heisenberg) spins, because the couplings J_{ij} are essentially real numbers. We shall see that, by going from a lattice to the continuum, and from a microscopic (spins) to a semi- macroscopic description of the matter field, a full exploitation of gauge invariance in disordered condensed matter (Yang-Mills theory) becomes possible.

This simple example (2.2) of a spin glass on a lattice emphasizes the main characteristics of gauge invariance in disordered systems:

a) Gauge invariance is an exact symmetry of H,

b) It preserves essential geometrical ingredients (frustration or odd lines).

c) It enables us to recover as much generative homogeneity as is compatible with (b), for example, by treating J as dynamical variables, and including (b) as constraints (source terms)[50]: From eq. (2.3), $Z \to \sum_{\{J\}=\pm J} Z[\{J\}]\, \delta\,(\mathit{frustration})$. An integral representation of the delta functions restores the full gauge invariance, at the price of a more complicated effective Hamiltonian.

2.2 - Gauge invariance at a semi-macroscopic scale as a genuine symmetry

It was argued in section 1.4 that the non-generative homogeneity of glasses, associated with randomness (non-collinearity of local reference frames), is a genuine, $SO(3)$ gauge symmetry. Indeed, as Jaynes has aptly put it in a different, but relevant context (the Bertrand "paradox" of probability theory), "Every circumstance left unspecified in the statement of a problem (here, the frames' orientations) defines an invariance property which the solution must have if there is to be any definite solution at all. The transformation group, which expresses these invariances mathematically (here, the gauge group of local rotations), imposes definite restrictions on the form of the solution, and in many cases fully determines it"[81]. Let us now be more specific.

The seminal 1978 paper of Dzyaloshinskii and Volovik (DV)[55] begins with the statement that the temptation to use the concept of

local exchange invariance to describe the spin glass state, is difficult to resist. Most readers did, I believe, agree immediately with this preamble, albeit for their own, different reasons, even though they did not accept at face value the specific model of DV.

Here were my own reasons: Elementary excitation are deviations of the spins, SiO_4 tetrapods, ... from the orientation of the local reference frame, and their (exchange, twist, ...) energy is given by comparing deviations at different points, each with a different frame orientation. The ordinary derivative ∂S, which measures these deviations in uniform magnets, must be replaced by a covariant derivative DS, with $D = \partial + iA$, where A is the connection or gauge field, which defines parallelism in the frames at two different points. The gauge field provides the answer to the technical problem of connecting points with different frames. The next step is to show that the particular orientation of the frame at a given point has no physical importante (gauge invariance).

Hertz[56] argues by analogy with ferro- and antiferromagnets: The exchange energy is given, typically, by $[(\partial - i\vec{Q})\phi]^2$, where ϕ is, for example, the angle of a XY spin, and $\vec{Q}$ is the wave vector of the magnetic modulation, $\vec{Q} = 0$ in ferromagnets, $\vec{Q} \neq 0$ in antiferromagnets (Ginzburg-Landau free energy). In spin glasses, $\vec{Q}(\vec{x})$ is a random variable with a given distribution; it is the gauge field or connection.

In fact, gauge invariance should occur whenever one can define noncollinear, local reference frames. Connection between neighbouring frames isdefined arcwise, by requiring that two overlapping neighbourhoods have local frames fitting together without any rotation. However, a finite circumnavigation does not necessarily restore the frame to its original orientation, it only does so in the absence of curvature, or of disclinations (Fig.7).

Consequently, the orientation of the local reference Frames cannot be defined uniquely everywhere in the presence of disclinations. It is locally arbitrary, but the physical properties of the system are independant of this arbitrariness, ie., invariant under a local rotation of the reference frame (given a connection between neighbouring frames), which is precisely a SO_3 gauge invariance.

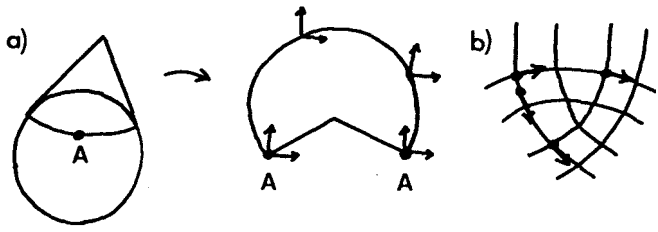

Fig.7. a) Example of parallel transport and non-unicity of the local reference frame in the presente of curvature. The frame in A has been rotated upon circumnavigation. The cone, tangent to the trajectory, can be flattened on a plane to define parallel transport. b) In a crystal, rotation of the reference frame must be an element of the space group.

Local frames occur in continuum elasticity theory. Glass can be regarded, on a semi-macroscopic scale (whenever all relevant length scales are longer than the interatomic distance a), as an isotropic, elastic continuum, with frozen-in interna1 stresses[40,57,58]. In metallic glasses, the stresses are due to the fact that Euclidean space cannot be filled by atomic configurations minimizing locally the energy (or maximizing packing: tetrahedra, icosahedra)[44,45]. In covalent glasses, there is an entropy barrier preventing crystallization (and inducing non-collinearity of the SiO_4 tetrapods, and stresses), when cooled from themelt. Thus, stresses are associated with non-collinearity of the frames, which are in turn relatedto disclinations or curvature[40,57,58]. Continuum elasticity is, accordingly, a gauge theory[60,40,57,58,59]. Unfortunately, almost no three-dimensional crystals have any disclination (because their strain energy is prohibitively high), so that, historically, the full gauge invariance of the theory was lost by the introduction of an *ad hoc,* distant parallelism (zero curvature, global reference orientation) hypothesis, justifiable in crystals, but not in glasses. This hypothesis breaks most of the gauge invariance of the theory at the onset. In glasses, dislocations screen the strain energy of disclinations (odd lines), so that they can exist on energy, as well as on topological grounds[40].

Comtet has found an explicit relation between integrability condition (connection) for frames on a minimal surface and the Euler--Lagrange equations of a class of two-dimensional SO_2 gauge field theories[61]. Gauge invariance of the field theory corresponds to rotation of the frames in the tangent plane of the surface. This relation can probably be generalized to three-dimensional, Yang-Mills (SO_3) field theory and the frames of three-dimensional hypersurface, thereby establishing explicitely the correspondance between non-collinear frames and SO_3 gauge invariance at the core of this discussion. As a bonus, the correspondance of Comtet requires the existance of an underlying curved hypersurface, which may turn out to be an explicit realization of the ideal, curved space of Kléman and Sadoc[44].

Gauge theory is therefore the proper method to go frorn a discrete lattice to the continuum, and in particular, to generalize the coupling J_{ij} to all points between i and j (which is easy to do if $J>0$, but not so if $J<0$). So, roughly, wehavesomematter field, coupled through a covariant derivative to a gauge field representing the coupling between spins. Specific questions remain:

i) Wat is the matter field?

ii) What is the gauge field, which replaces $\{J\}$ in the continuum?

iii) How should the disorder be quenched ?

The answer to (i) was an important idea of DV[55]. The matter field $\hat{\Phi}(\vec{x})$ represents, not one single spin, but a group of spins within an elementary cube of the discrete lattice centered at $\vec{x}$ (semi-macroscopic representation). Because frustration induces non-collinearity of the spins, $\hat{\Phi}$ is no longer a vector of given length (with values on a sphere (Heisenberg spins) or a circle (XY spins)), but a hedgehog, or hirsute object, whose manifold of states is that of the full rotation group SO_3 (Heisenberg) or SO_2 (XY). Similarly, in glasses, $\hat{\Phi}(\vec{x})$ is an object living in the full rotation group SO„ rather than a single tetrapod (E SO_3/T, where T is the tetrahedral group), for covalent glasses, or a single icosahedron (ϵ SO_3/I, where I is the icosahedral group), for metallic glasses. This is because the field $\hat{\Phi}$ must be defined everywherein a continuous space, and not only at the centre of the tetrapod or icosahedron.

In fact, $\hat{\Phi}(x)$ must be chosen so that it yields the correct

"defects" (vortices, frustration, odd lines)[62]. Heisenberg spins would not have given any frustration ($\pi_1(S_2) = 1$). Similarly, single tetrapods, tetrahedra or icosahedra would have given rise to line defects which would have been topologically entangled (since their respective π_1 are non-abelian[63]), thereby preventing the material to flow, so that the *same* model of the structure of glass could not describe the dynamics of its supercooled or viscous liquid, even though both states have the same structure. [At any rate, there is no generative tetrahedral or icosahedral symmetry in the glass, hence no reason to restrict the manifold of $\hat{\Phi}$ to a coset of SO_3].Hydrodynamics (irrotational fluids have for field a scalar potential $\phi(x)$, with velocity $\vec{v} = \vec{\nabla}\phi$, to be replaced by $\vec{v}$ itself when the field is rotational (with $\vec{w}$ = curl $\vec{v}$ as vortex density)), electromagnetism without, or with magnetic monopoles ($\vec{A}$ replaced by $\vec{B}$ = curl $\vec{A}$ as the field), and continuum elasticity without, or with disclinations[58], provide classical examples of the overriding influence of the defects on the selection of the proper matter field. Cf. also our introductory remarks (section 1.1).

Consequently, the matter field can be expressed in terms of a rotation operator $\hat{\Omega}$, $\hat{\Omega}^+ = \hat{\Omega}^{-1}$,

$$\hat{\Phi}(\vec{x}) = \lambda(\vec{x})\hat{\Omega}(\vec{x}) \tag{2.4}$$

(Stueckelberg decomposition). Whereas in spin glasses, the amplitude $\lambda(\vec{x})$ can be regarded as the order parameter[64] which vanishes at the spin glass transition, in glasses, it represents the size of the tetrapods and can be taken as a constant, A, everywhere exceptatthe core of the odd lines'where it vanishes. The characteristic length associated with fluctuations in h is $\xi \approx a$, the interatomic spacing in the network or the size of a plaquette. $\lambda \neq 0$ corresponds to the chemical properties of the constituting atoms, and is taken for granted at all temperatures relevant for the glassy, liquid or solid states. This approximation is sometimes referred to as the nonlinear σ model.

(ii) We postpone discussion of the precise meaning of the gauge field $\hat{A}_\mu(\vec{x})$ unti1 the next part (eq. 3.2), apart from remarking that it should appear naturally and automatically in the free energy density through the covariant derivative of the matter field, and that it is directly related to the non-collinearity of the tetrapods. In

fact, introduction of a gauge field $\hat{A}_\mu(\vec{x})$ is *necessary* to make the derivative covariant (eq. *2.6* below). As it is its only physical purpose, one can assume that the covariant derivative also provides the *only* coupling between gauge and matter field (minimal coupling). The length scale of the gauge field, l, (penetration depth in superconductors) is the range of non-collinearity. Thus (see Pl.1), $l >> \xi \approx a$, and glasses are type II gauge materiais (in the superconductivity terminology). They exhibit vortices rather than full Meissner effect.

(iii) From our experience with discrete lattices (end of section 2.1), it seems evident that gauge field should be treated as dynamical variables (and full gauge invariance or homogeneity maintained) as much as possible. Only the *source* of gauge fields (the frustration or odd lines), ie., the essential disorder, need be quenched. This remark is in contrast with the assumptions of DV and of Hertz, who both felt that *all* disorder terms should be quenched. Hertz[56] quenches the gauge field $\hat{A}(\vec{x})$, and DV[55] give it a mass term in the free energy. Both procedures *break* gauge invariance. Ours is gauge invariant. Furthermore, the sources of gauge field - the (geometrical) odd lines, quenched below T_0 in glasses, and at all temperatures in spin glasses - can be treated simply as punctures of the space C into which matter and gauge fields are put, exactly like flux lines in extreme type II superconductors. Boundary conditions on the puncture are free. This allows gauge and matter field (with amplitude $\lambda = cst$) to take up configurations (eg. rotated by 2π around the puncture), which would have been forbidden if the space had been simply-connected. Thus, we replace a simply-connected, Euclidean space by a punctured one (Σ). This complicates slightly the geometry but simplifies enormously the algebi-a, notably by letting $\lambda = |\hat{\Phi}| = cst$ everywhere in C, and by restoring full gauge invariance to the system within C.

For example, consider a superconducting ring C. The free energy within C is gauge invariant, themagnitude of the matter field (superconducting order parameter) is uniform within C, and the new configurations associated with multiple-connectivity are those of quantized fluxoid. The degeneracy between these configurations is only lifted if the (electromagnetic) free energy outside C (chiefly inside the ring's hole) is included.

In summary, sources of gauge field are punctures, with free boundary conditions (except that every configuration must be single-valued, and rotate by a multiple of 2π about every puncture). The free energy is fully gauge invariant in punctured space C, where the magnitude of the matter field can be taken as constant. The multiple-connectivity of C implies that there are several possible ground states (valleys), all degenerate because they are related to each other by gauge transformations (see part III), instead of the unique ground state in simply-connected space, which is one of the cornerstones of classical solid state physics.

2.3 - Gauge invariant model free energy for glass

Without further ado, we can now write down the model free energy for glass[37].

$$F = \int_{\Sigma} d\vec{x}\, f(\vec{x})$$

$$f(\vec{x}) = \frac{1}{2}\,\mathrm{Tr}\{\gamma\left[(D_\mu\hat{\Phi})\,(D^\mu\hat{\Phi})^+\right] + \frac{1}{2}\left[\hat{F}_{\mu\nu}\hat{F}^{\mu\nu}\right]\}$$

$$D_\mu\hat{\Phi} = \partial_\mu\hat{\Phi} + g\left[\hat{A}_\mu,\hat{\Phi}\right]$$

$$\hat{\Phi}(\vec{x}) = \lambda_0\hat{\Omega}(\vec{x}) \quad , \quad \hat{\Omega}^+ = \hat{\Omega}^{-1}$$

$$\hat{F}_{\mu\nu} = \partial_\mu\hat{A}_\nu - \partial_\nu\hat{A}_\mu + g\left[\hat{A}_\mu,\hat{A}_\nu\right] \qquad (2.5)$$

where C is the Euclidean space, punctured by odd lines, with free boundary conditions.

$f(\vec{x})$ is invariant under gauge transformations, the *local* rotations $\hat{U}(\vec{x})$, $\hat{U}^+ = \hat{U}^{-1}$,

$$\hat{\Phi}' = \hat{U}\hat{\Phi}\hat{U}^{-1}$$

$$\hat{A}'_\mu = \hat{U}\hat{A}_\mu\hat{U}^{-1} + \frac{1}{g}\,\hat{U}(\partial_\mu\hat{U}^{-1}) \qquad (2.6)$$

under which the derivative is covariant,

$$(D_\mu\hat{\Phi})' = \hat{U}(D_\mu\hat{\Phi})\hat{U}^{-1}$$

$\hat{F}_{\mu\nu}$ is gauge covariant,

$$\hat{F}_{\mu\nu}' = \hat{U}\hat{F}_{\mu\nu}\hat{U}^{-1} \qquad (2.7)$$

(unlike its abelian counterpart, the electromagnetic induction $\vec{B}=\mathrm{curl}\,\vec{A}$, which is gauge invariant), and is therefore only related to the non-collinearity density $\tilde{F}_{\mu\nu}$, a physical observable which must be gauge invariant (eq.3.2).

Free energy (2.5) was written down as early as 1954 by Yang and Mills[65] in the completely different context of elementary particles. This suggests that there is little arbitrariness in the selection of a gauge invariant free energy.

Gauge invariance imposes the introduction of a new field, the gauge field. On the other hand, it severely restricts the possible free energy densities. Consequently, eq. (2.5) has very little arbitrariness: Only,

1. minimal coupling between gauge ($\hat{A}_\mu$) and matter ($\hat{\Omega}$) field (solely through the covariant derivative),
2. one energy (density) scale $\varepsilon = (\gamma\lambda_0^2 g)^2 = 1/(g^2\ell^4) = k_B T_0/\ell^3$,
3. one length scale (the penetration depth) $\ell = 1/(\sqrt{\lambda}g\lambda_0)$,
4. the distance ζ between punctures ($\ell >> \zeta >> \xi \approx a$), and their configuration (semi-dilute),

have or will be chosen on physical grounds.

Odd lines, and gauge invariance will enable us to construct explicitely the many valleys and two-level systems responsible for the low-temperature properties of glasses[2,5-7].

III – TUNNELING MODES

3.1 - Many potential valleys in configuration space

The anomalous properties of glasses at low temperatures, briefly reviewed in section 1.2.a, and in detail in refs. [2] and [5], are properly described by the concept of tunneling modes[6], which are theelementary excitations of systems with several deep potential minima in configuration space. In this part, I shall use the model free energy (2.5), ie. odd lines and gauge invariance, to locate pre-

cisely the many valleys in configuration space, to label them, and to calculate the tunneling rate between different valleys.

It is elementary to show that a distribution $N(\Delta_0)$ of two-level systems (2LS) split by an energy Δ_0 (proportional to the tunneling rate), yields a specific heat increasing linearly with temperature,

$$C = \frac{\pi^2}{3} k_B^2 N(0) T$$

(assembly of Fermi-Dirac oscillators), where k_B is Boltzmann's constant, as long as the density of two-level systems remains finite as $\Delta_0 \to 0$. The coefficient $C/T \approx 10^{-6} Wsg^{-1}K^{-2}$ is typically an order of magnitude smaller than that of a good metal ($\approx 10^{-5} Wsg^{-1}K^{-2}$ for Cu), suggesting 10^{-5}-10^{-6} 2LS / atom active at $\approx 1K$, with a size of ≈ 40 Å, since resonance (T_2) measurements indicate that the 2LS are roughly independent excitations[2,105].

Three remarks can be made at the onset:

1) In tunneling modes, the higher and broader the potential barrier, the smaller the tunneling rate and the level splitting. In glasses, splittings down to $\approx (10^{-2}K) k_B$ are observed (no departure from linearity, or time dependance of the specific heat down to these temperatures), suggesting high ($\approx k_B T_0$) and broad potential barriers, that is a lot of atoms moving very little. The size of 2LS indicates that, as far as quantum coherence goes, they are semi-macroscopic: considerably larger than a single electron or alpha particle, but still smaller than a SQUID or Schrödinger's cat.

2) The classical potential barrier may even be infinite (and will be so for our continuum model free energy (2.5)), but, as long as $\sqrt{V}$ is integrable, the tunneling rate remains finite. Then, the 2LS have no classical equivalent. This may explain why the explicit nature of tunneling modes has remained elusive for 10 years.

3) Saturability[5], and coherence[7] of the 2LS indicate that the elementary excitations within each potential well are thermally inaccessible below $\approx 1K$. They lie at much higher energies than the splitting Δ_0 between ground states of different wells. Thus, only the ground state within each well is relevant to the physics of glass at low temperatures. The situation is reminiscent of the tight-binding, or LCAO model of electronic band structure of metals and molecules, where only

one orbital per atom is relevant to the physical or chemical properties in a limited energy range, from which core levels, and higher atomic excited states, are inaccessible.

These remarks are sketched in Fig. 8, which is also an adequate summary of the conclusions of this part.

The specific heat is approximately linear in the range $0.025K$-$1K$. This suggests a constant density of states for 2LS, $N(\Delta_0) = N(0)$, in this energy range. In fact, Lasjaunias *et al*[66] havesuggested that $N(\Delta_0)$ has a gap below 16 $mK.k_B$, thereby giving a limit for the slowest tunneling rate observable experimentally. It must be emphasized that severa1 problems of detail remain with the tunneling mode concept (only approximate linearity of C, T^3 contribution to C significantly above that expected from Debye phonons, response of the system to short thermal pulses, etc[67,68,105]), but the major theoretical challenge is universality: "...no plausible argument has been presented yet why all amorphous substances have approximately the same density of states of tunneling defects which, and that is probably even more puzzling, scatter the phonons with almost equal strength"[67]. The experimental situation will also be clarified, as new and direct methods if investigation and comparison are developed (effects of high pressure[68], or, as in epoxy resins, of the size of the network constituents[69]).

3.2 - Classical, ground state configurations

According to Fig.8, it is sufficient to identify and label the ground state or metastable configuration of every valley. These ground state configurations $\{\hat{A}_\mu, \hat{\Omega}\}$ are classical solutions of the Euler-Lagrange (EL) equations obtained by minimizing the free energy (2.5) in *punctured* space C (the punctures being put in a *priori* - quenched at random below T_0), with free boundary conditions on the puncture. Free energy, boundary conditions, and EL equations, are all gauge invariant. The EL equations look frighteningly complicated[37], but we shall not need an explicit solution.

The matter field $\hat{\Omega}$ is obviously parametrized by rotations, and one anticipates two ground state configurations per puncture, one corresponding to a rotation of $\hat{\Omega}$ upon circumnavigation around the puncture

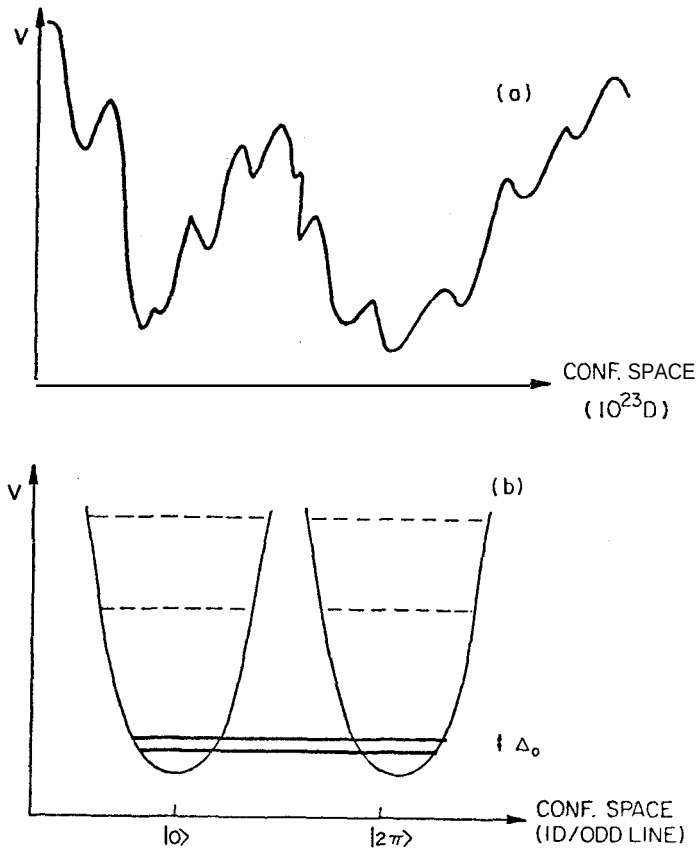

Fig.8 - The many valleys in configuration space, giving rire to tunneling modes. a) Old picture (ref. [6]). b) New picture (this paper). Note that the 10^{23}-dimensional configuration space has been reduced to 1D per odd line; the valleys (topological sectors) can be labelled ($|0\rangle$, $|2\pi\rangle$), and their distance (or the energy splitting A) calculated. Dotted lines: excited states in each sector (irrelevant at low T). Full lines: 2LS. Only a rough topography of the valleys is required to obtain ground state and elementary excitations of a glass.

by 0 or a multiple of 4π, the other to rotation by an odd multiple of 2π. (The latter is the new configuration permitted by the multiple-connectivity of C). All other configurations can be continuously deformed into these two. (Recall our discussion of section 1.6, and the fact that the rotation group is not simply connected ($\pi_1(SO_3) = Z_2$), necessary to justify quantization of the electron's spin in half integral multiples of $h/2\pi$). We must show that the gauge field $\hat{A}_\mu$ is *also* parametrired by rotations. Then, we will have proven that thereare *two* ground state configurations per puncture, parametrized by rotations.

To do so, we construct a linear combination of matter and gauge fields which is gauge *invariant*, so that a covariant gauge transformation (rotation) of the matter field $\hat{\Omega}$ induces a contravariant rotation of the gauge field. This procedure is familiar in superconductivity and electromagnetism, where the phase θ of the order parameter $\psi(\vec{x}) = \rho(\vec{x}) \exp[\theta(\vec{x})]$ forms with the vector potential $\vec{A}(\vec{x})$, the gauge invariant combination $\vec{C}(\vec{x}) = \vec{A}(\vec{x}) - (hc/2\pi e)\nabla\theta(\vec{x})$

$$\vec{A}' = \vec{A} + \nabla\chi$$

$$\theta' = \theta - (hc/2\pi e)\chi$$

$$\vec{C}' = \vec{C}$$

(This constitutes also the simplest derivation of the Higgs mechanism (massive vector boson) in minimally coupled, abelian gauge theories).

The construction proceeds in a few steps:[37,58]

i) A *given* configuration of the matter in C can be written in terms of its orientation at some point $\vec{x}_0$, $\hat{\Omega}_0 = \hat{\Omega}(\vec{x}_0)$, and a rotation operator $\hat{W}(\vec{x}) \in SO_3$, which is independant of the path from $\vec{x}_0$ to $\vec{x}$, apart from a winding number (rotation by $2\pi n$, $n = 0,1$) around every puncture. Then, $\hat{\Omega}(\vec{x}) = \hat{W}(\vec{x})\hat{\Omega}_0\hat{W}^{-1}(\vec{x})$, and the "phase gradient" (the phase orientation density $\hat{\chi}_\mu = (\partial_\mu W)W^{-1}$) are path-independant.

ii) One then goes to a rotated frame, defined by $\tilde{\Lambda} = \hat{W}^{-1}\hat{\Lambda}\hat{W}$, for any operator $\hat{\Lambda}$. The new covariant derivative $\tilde{D}_\mu\tilde{\Lambda} = \hat{W}^{-1}(\hat{D}_\mu$, involves the phase $\hat{\chi}_\mu$ and the gauge field $\hat{A}_\mu$, in a linear combination $\tilde{C}_\mu$, (Stueckelberg decomposition)

$$\tilde{D}_\mu = \partial_\mu\hat{1} + [\tilde{C}_\mu,$$

$$\tilde{C}_\mu(\vec{x}) = g\tilde{A}_\mu(\vec{x}) + \tilde{\chi}_\mu(\vec{x}) = [\tilde{C}_\mu(\vec{x})]' \qquad (3.1)$$

which is *gauge invariant*, as is any operator $\tilde{A}$ in the rotated frame. (Under gauge transformation $\hat{U}(x)$, $\hat{W}'(x) = \hat{U}(x)\hat{W}(x)$, and $\hat{\Lambda}' = \hat{U}\hat{\Lambda}\hat{U}^{-1}$ implies $\tilde{\Lambda}' = \tilde{\Lambda}$). This includes $\tilde{F}_{\mu\nu}$,

$$g\tilde{F}_{\mu\nu} = \partial_\mu \tilde{C}_\nu - \partial_\nu \tilde{C}_\mu + [\tilde{C}_\mu, \tilde{C}_\nu] = g\tilde{F}_{\mu\nu}' \tag{3.2}$$

which, being gauge invariant, measures the physical density of non-collinearity. Similarly, the free energy density (2.5) can be written in term of the gauge invariant $\tilde{C}_\mu$,

$$f(\vec{x}) = \frac{1}{2}\,\mathrm{Tr}\{\gamma\lambda_0^2[\tilde{C}_\mu, \hat{\Omega}_0][\tilde{C}^\mu, \hat{\Omega}_0]^+ + \frac{1}{2}\tilde{F}_{\mu\nu}\tilde{F}^{\mu\nu}\} = f(\vec{x})' \tag{3.3}$$

iii) The combined gauge field $\tilde{C}_\mu$ is accordingly gauge invariant, and therefore unique. The rotation $\hat{W}(\vec{x})$, which parametrizes the matter field $\hat{\chi}_\mu$ or $\hat{\Omega}$, also parametrizes the gauge field $\hat{A}_\mu$. Because there are only two possible configurations per puncture of the matter field, up to continuous deformations, corresponding to rotation by 0 or 2π, there are also two configurations of the gauge field, and therefore, two ground state configurations per puncture $\{\hat{\Omega}, \hat{A}_\mu\}$, solutions of the EL equations for the free energy F in punctured space C. q.e.d.

Invariance of the free energy under a non-trivial gaugetransformation (rotation by 2π), implies that F is periodic in the flux triggering the gauge transformation, as long as the source of non-collinearity vanishes in C (cf. superconducting ring, where F is periodic in the applied magnetic flux, as long as the *applied* magnetic induction vanishes inside the superconductor). This generalizes Bloch's theorem for superconductors[26], to any minimally coupled gauge theory.

Similarly, the restriction on the matter field (which must be uniform for a given configuration, ie. returned to the same orientation after circumnavigation), translated into a restriction on the gauge field, corresponds to fluxoid quantization in superconductors. It is a direct consequence, in minimally coupled gauge theories, of the non-triviality of some gauge transformations.

3.3 - Tunneling states, two-level systems

We have identified and labelled two ground state configurations per puncture (odd line), which will serve as the "atomic or-

bitals" of our LCAO. These two "tunneling states" $|0\rangle$ and $|2\pi\rangle$ are characterized by rotations of 0 and 2π upon circumnavigation about the puncture. They are degenerate in energy (by gauge invariance of F). But neither classical configuration is gauge invariant, and can qualify as the true ground state of the glass, which must be gauge invariant. (There is no reason to assume that gauge invariance should be broken in glasses, as we have argued in part II). Tunneling, however slow, must take place to restore gauge invariance. The true ground state and elementary excitation, per odd line, are the gauge invariant combinations,

$$|\pm\rangle = \frac{1}{\sqrt{2}} \left[|0\rangle \pm |2\pi\rangle \right] \tag{3.4}$$

which are the 2LS, split by $(\hbar/2\pi)$ times the tunneling rate.

3.4 - Tunneling rate

We shall assume that the frozen configuration of punctures is semi-dilute, that is, intermediate between dilute (alphabet soup), and melt (dense spaghetti bundles) (The appellation is borrowed from polymer physics and may not correspond to gastronomic states). In this case, only one length describes the frozen, isotropic configuration, the distance ζ between non-adjacent segments of odd lines (which may equally well belong to the same or to different odd lines). Thus, to transform configuration $|0\rangle$ into $|2\pi\rangle$ about a given odd line, it is sufficient for a quantum flux of rotation of length ζ to tunnel through a distance ζ only. Further away lies the region influenced by other odd lines.

Justification for a semi-dilute distribution relies either on the dynamics of odd lines when the glass is cooled from the melt (part IV), or on maximizing the entropy (most probable distribution)[57]. Qualitatively, the most probable distribution of odd lines is that which maximizes the density of low-energy states, per unit volume and energy interval. This suggests the semi-dilute distribution, in which the loops are concentrated enough for the odd lines to intertwine and the nearest non-adjacent segment to belong to another loop (maximum number of 2LS per unit volume), but not concentrated enough that their cores overlap (maximum number of 2LS per energy interval). This picture has not yet been confirmed experimentally.

The energy splitting A, is given by the transition amplitude,

$$\frac{\pi\Delta_0}{k_B T_0} = \langle 0|2\pi\rangle = \int [D\hat{\Omega}]\,[D\hat{A}_\mu]\, \exp\{-(2\pi/\hbar) \int d\tau\ L(\tau)\} \qquad (3.5)$$

for all paths in imaginary time τ connecting $|0\rangle$ and $|2\pi\rangle$, where $L(\tau)$ is the Lagrangian, and the energy has been adjusted to vanish at the initial and final configurations. The leading contribution to Δ_0 is given by the classical paths from $|0\rangle$ to $|2\pi\rangle$ minimizing the exponent (action) in (3.5). One faces, at once, two major problems: 1) To obtain a Lagrangian from the free energy (2.5), ie. dynamics from thermodynamics. 2) There are no continuous, classical paths from $|0\rangle$ to $|2\pi\rangle$, since the configurations are not homotopic. A trick must be used:

For a semi-dilute distribution of odd lines $l \gg \zeta \gg a$, the free energy (2.5) or (3.3) can be linearized (the free energy is dominated by terms with the highest power in l, that is the linear terms in $\tilde{C}_\mu$ in $\tilde{F}_{\mu\nu}$, because the length scale of $\partial\tilde{C}$ is now ζ rather than l as for a single odd line or in the dilute limit $\zeta > l$). The linearized free energy is similar to that of an extreme type II superconductor, with penetration depth l and constant magnitude of the order parameter. Δ_0 will therefore be given by the tunneling rate of a flux quantum across a superconducting ring of radius ζ, height ζ and radius of puncture a. This rate can then be evaluated by opening a thin slit (width a) across the cylinder. This trick provides at a stroke 1) a Lagrangian, 2) a classical path.

One has, in fact, the geometry of a Josephson transmission line, along which the magnetic flux satisfies a sine-Gordon equation[70], whose Lagrangian is well-known

$$L(\tau) = -k_B T_0 \zeta \int dy \left[\frac{1}{2\bar{c}^2}(\partial_\tau\phi)^2 + \frac{1}{2}(\partial_y\phi)^2 - \frac{\cos\phi - 1}{\lambda_J^2}\right] \qquad (3.6)$$

where λ_J is the Josephson penetration depth and $\bar{c}$, the wavefront velocity. For a thin slit of width a, $\lambda_J \approx l$, and $\bar{c} \approx c\sqrt{a/(2\zeta)}$.

A typical superconducting ring has heigh L, radius ζ, and $L > \zeta \gg \lambda_J$, so that a tall, thin soliton propagates along a long slit. The

cosine term dominates the dynamics, and the tunneling amplitude goes as $\exp[-\text{cst } L\zeta]$ which is utterly negligible, so that superconducting magnets can hold their magnetic field for long enough to be usefiil.

By contrast, in glass, the rotation flux quantum is a very fat $\lambda_J = l$, short (height ζ) object, which has to move very little (distance $\zeta << l$). The $[\cos\phi - 1]/\lambda_J$ term is negligible, and $\int d\tau\, L(\tau) \approx$ the energy of a 2D vortex. The tunneling amplitude is much larger[58],

$$\Delta_0 = \frac{k_B T_0}{\pi} \exp\left[-D(\zeta/a)\ln(\zeta/a)\right] \tag{3.7}$$

as long as ζ is not macroscopic (semi-dilute limit). Here $D = 16\pi^2 k_B T_0 a/(hc)$.

Typically, $\zeta/a \approx 40$, $T_0 \approx 300K$, $(hc/2\pi k_B T_0) \approx 10^5$, yielding an exponent $\approx 1/2$. Also, a distribution of distances ζ,

$$P(\zeta) \approx (D/a\pi)\left[1 + \ln(\zeta/a)\right] \exp\left[-D(\zeta/a)\ln(\zeta/a)\right]$$

corresponds to a flat and broad density of 2LS energies $N(\Delta_0) \approx (k_B T_0)^{-1}$ for $\Delta < k_B T_0$. Numbers obtained from (3.7) are therefore reasoriable. Note that the density of 2LS $N(\Delta_0)$, is inversely proportional to the only energy scale of the problem $k_B T_0$ (see eq. (2.5)). Thus, in glass, tunneling does occur, and yields the dominant excitations below some low temperature proportional to $1/\sqrt{k_B T_0}$. This temperature may be anomalously low if the elastic energy $k_B T_0$ is large, as is the case in a-Ge, or if the distribution of odd lines is not semi-dilute. On the other hand, no odd lines, and no tunneling modes are expected in glasses which can be described by a bichromatic model containing even rings only[71], or its continuous equivalent, a pure gauge model. *a-GaAs* may be a system without odd member rings, as long as wrong bonds (As-As or Ga-Ga) are excluded by electronegativity.

The density of 2LS is inversely proportional to the only energy scale of the problem $k_B T_0$. (Cohen and Grest also obtain this relation in their free volume + percolation model[72]). This should be directly observable by comparing viscosity and low T properties of the same system under pressure. Measurements by Bartell and Hunklinger[68] in

vitreous SiO_2 show that the low temperature ultrasonic attenuation (ie. the density of 2LS) surprisingly increases with increasing pressure. This is consistent with the anomalous pressure dependance of the viscosity (which decreases as p increases) observed in GeO_2 (and SiO_2 is expected to follow the same behaviour[73], to the delight of geologists, worried about the viscosity of the earth's mantle) through T_0 decreasing with pressure (although why this is so, is not clear miscroscopically). On the other hand, neutron *irradiated* silica apparently follows the opposite, less unexpected, trend: Increase of the mass density upon irradiation is accompanied by a decrease in the density of 2LS, $N(\Delta_0)$, ie. an increase of the thermal conductivity and a decrease of and specific heat[74].

However, irradiated and fused silica have strikingly different structural characteristics, even if they are both amorphous. (The intensity of the 609 cm^{-1} (sharp) Raman line of fused silica increases by an order of magnitude upon irradiation[75]).

3.5 - Can one see what it is that tunnels ?

A superconducting ring can be prepared in one of its free energy minima because an externa1 magnetic flux is readily available from a magnet. Tunneling between energy minima is then observed as Josephson effect. In glass, by contrast, rotation flux does not correspond to a commercially available knob. However, there exist a rnethod to prepare the system in one of its classical ground states, which takes advantages of the coherence of tunneling between two levels, the *phonon* or *electric* (when the 2LS have a dipole moment) echoes[7], the 2LS counterparts of spin (S = 1/21 - echo spectroscopy in magnetic resonance.

In order to find out precisely what it is that tunnels, one would like to tune a structural probe (pulsed neutron beam) to the coherently oscillating tunneling modes, so that neutrons take successive snapshots of the 2LS when they are in the classical state $|0\rangle$, say. Constructive interference between successive snapshots can be arranged by splitting the neutron beam, scattering beam 1 on the sample at time t=0, when the 2LS are in the classical state $|0\rangle = (1/\sqrt{2})\,[|+\rangle + |-\rangle]$, then

delaying the scattered beam, while beam 2 is first delayed, then scattered by the sample at time $t=2t_0$ when the 2LS are again in state $|0>$. The two beams are combined at some later time $t > 2t_0$, and superposition of neutron diffraction of the same 2LS in the same, classical state $|0>$, should show constructive interference[76]. (Fig.9). Varying the delay time detunes neutron and 2LS, and leads to destructive interference between scattered beams. Varying the time of scattering of the first beam (taken above to be $t=0$), will find the 2LS outside the classical state, within the barrier, and the constructive interference of the scattered beams destroyed. (Even though neutrons are quantum probes, which could couple to 2LS through the off-diagonal operators σ_z or σ_y, as well as through the diagonal ones, $\hat{1}$ or σ_z, the 2LS involve too many atoms in a disordered configuration, to be detected by neutrons as anything else than density fluctuations (through operator $\hat{1}$). In this case, echo (coherence) is observed only for the classical states $|0>$ and $|2\pi>$ (eq. 3.8)). Combination of constructive and destructive interferences should fingerprint what it is that tunnels.

Phonon echoes are obtained as follows: One applies to the 2LS, described by the Hamiltonian

$$H_0 = -\frac{1}{2}\Delta_0\,\sigma_z$$

($|\pm>$ are eigenvectors of σ_z), two high amplitude, A_1, electrical or acoustic pulses of duration τ (SET pulse) and 2τ (REVERSE pulse), respectively. The frequency $A = \omega(h/2\pi)$ of the pulses should be $\approx\Delta_0$ ($<<\Delta_1$), for resonance.

$$H_1(t) = \frac{1}{2}\Delta_1(\sigma_z \cos\omega t + \sigma_Y \sin\omega t)$$

The SET pulse induces a phase shift

$$S \approx \sqrt{(\Delta-\Delta_0)^2 + \Delta_1^2}\,\tau\,(2\pi/h) \approx \Delta_1\,\tau\,(2\pi/h) = \pi/4$$

The evolution of the 2LS is evaluated in a rotating frame, where the effective Hamiltonian is time-independant. The time-table of the tuned echo-neutron pulse system is sketched in Fig. 9. A $\pi/4$ pulse prepares the 2LS in classical state $|0\rangle$ at $t=0$. A $\pi/2$ pulse at $t=t_0$ reverses the 2LS state, from $a|+\rangle + b|-\rangle$ to $a|-\rangle + b|+\rangle$. The echo is observed at $t = 2t_0 + 2\tau \approx 2t_0$, when the 2LS is again in the classical state $|0\rangle$. The two pulsed neutron beams (*) measure the state of the system at t=O and $2t_0 + 2\tau$.

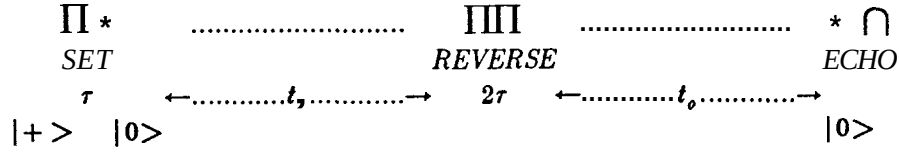

Fig.9. Time-table of the tuned 2LS echo-neutron system

A distribution of 2LS $\{\Delta_0\}$ stills shows coherence (echo), as long as the reverse pulse is short compared to the time of free propagation $\Delta\tau << \Delta_0 t_0$, and the 2LS are initially in a classical state:

$$|+/-\rangle (at\ t=O) \rightarrow C(-/+\rangle + t_0\text{-}dependant\ term\ (at\ t=t_0+2\tau) \quad (3.8)$$

Thus,

$$|+\rangle \pm |-\rangle\ (at\ t=0) \rightarrow \pm\, C(|+\rangle \pm |-\rangle) + incoherent\ terms\ (at\ t=t_0+2\tau)$$

where $C = i\sin(2\mathcal{S})\sin\theta$ and $\mathcal{S} = \tan^{-1}\frac{}{A-A_0}$. Maximum coherence occurs at resonance $A \approx \Delta_0$, where $2\mathcal{S} = \theta = \pi/2$

In this part, we have exhibited explicitely the many potential valleys in a continuous model of glass. The situation is sum-

marized in Fig. 8. Some progress has recently been made towards repeating the same analysis for discrete random networks, and obtaining again two classical configurations per odd lines[77].

IV - SUPERCOOLED LIQUID AND GLASS TRANSITION

4.1 - Introduction

This part will be concerned with the regime $T > T_0$ above the glass transition temperature, where the structure can be deformed under shear, and glass behaves like a supercooled, highly viscous liquid instead of a structurally invariant, elastic solid below T_0. Viscosity, or any inverse structural relaxation rate, follows the empirical Vogel-Fulcher relation (1.1), at least approximately, as described in detail in section 1.2b.

Above T_0, odd lines can moves as the structure is deformed. However, they obey a topological conservation law (section 1.6), so that they can expand or shrink, but remain uninterrupted, assuming as before that bonds are broken and reconstructed over a much shorter time scale than that associated with the fluidity. Odd lines are the slow - or hydrodynamic modes of the system. Viscosity, or any structural relaxation rate, is associated with the diffusion of some "defect", in the crude but adequate model of Glarum, and Phillips, Barlow and Lamb[78]. The "defect" must be of sufficient generality to account for the universality of the relaxation process in glass, and of sufficient stability to retain its identity and avoid disintegrating during (slow) diffusion. Odd lines, or 2π-disclinations, as the only structurally stable ingredients of any glass, clearly fill the bill on both counts. Free volume would not, on its own, be stable enough.

The glass transition at T_0 corresponds to the freezing or "condensation" of the odd lines. We know already (section 2.2), that glass transition does not correspond to a vanishing amplitude of some order parameter (unlike the transition in spin glasses), nor to the breaking of some (gauge) symmetry. A mean field calculation of the density of free, or mobile odd lines will yield a condensation similar to the Kosterlitz-Thouless transition, but in 3D, which may be frustrated close to T_0 by a crossover to Arrhenius behaviour (see section 4.5).

Ideally, one would like to start from the free energy (2.5), and allowing the punctures to move freely, like vortices in hydrodynamics and flux lines in superconductivity. Unfortunately, to the best of my knowledge, nomethod has been found as yet to isolate the "vortices" as elementary excitations of a field theory in the continuum, similar to the Villain method on lattices[79]. [In electromagnetism, this would mean partitioning the integral over all gauge field configurations $A(x)$ into a discrete sum over configurations of different, quantized flux $\oint \vec{A}(\vec{x})\, d\vec{x}$]. We must therefore calculate the energy E and entropy S of an assembly of free (mobile) odd lines of density ρ_f. Minimization of the free energy $F[\rho_f] = E[\rho_f] - TS[\rho_f]$, $\delta F/\delta \rho_f = 0$, yields the density of *free* odd lines in thermodynamic equilibrium $\rho_f(T)$. A semi-dilute distribution of odd lines, has their dimensionless density related to their shortest mutual distance ζ by

$$\rho = (a/\zeta)^2 \tag{4.1}$$

This is a pedestrian treatment of the model free energy (2.5) at high temperatures when the punctures are mobile, but it is the best we can do. The argument was first sketched by Anderson[1], and worked out in ref. [86].

This method has the free odd lines as the only (slow) dynamical variables of degrees of freedom, through their density ρ_f. The other (frozen) odd lines do not contribute to the dynamics and thermodynamics as a first approximation. They cannot be displaced or adjusted to lower the free energy of the system. At T_0, all odd lines are frozen $\rho_f(T_0) = 0$ (eq. 4.5). Just above T_0, there are so few free odd lines that they form a dilute distribution, even though the configuration of *all* odd lines, frozen and free, is semi-dilute at all temperatures, as discussed in section 3.4.

All the results of this part have also been obtained from continuum elasticity theory, allowing for (2π-) disclinations, which are, as we have seen in section 1.6, the only topologically stable, line constituents in a medium with trivial space group. Dislocations are not topologically stable, and screen the strain energy of disclinations, which are then allowed to exist in 3D glasses on energy grounds (their strain energy is unacceptably high in crystals, where it *increases* linearly with the distance between two disclinations). Most of the con-

tinuum elasticity results on glass are due to Duffy, and have been published extensively[40,80,57].

4.2 - Energy of an assembly of odd lines

We start with the fields and geometry of free energy (2.5) or (3.3). Assuming (to be confirmed a *posteriori*) a semi-dilute distribution of free odd lines at $T >> T_0$, $\zeta << l$ (where l is the length scale of the gauge field, which measures the range of non-collinearity), we can linearize the theory. The quartic terms in the free energy density (2.5) or (3.3) are negligible when compared to the quadratic terms involving spatial derivatives, because, in terms of rescaled gauge fields $\bar{C}_\mu = l.\tilde{C}_\mu$,

$$l\partial\bar{C} \approx l/\zeta >> \bar{C} = 1$$

The free energy density (3.3) reduces to

$$f(\vec{x}) \approx \frac{1}{2} \varepsilon \mathrm{Tr}\{l^2 (\mathrm{curl}\ \bar{C})^2\} + \sum_i e_{\mathrm{core}\ i}\ , \qquad (4.2)$$

which is that of electromagnetism of current loops (apart from the fact (taken care of in the trace) that $\bar{C}$ is a tensor rather than a vector). In particular, the Euler-Lagrange equations become simply

$$\mathrm{curl}\ \mathrm{curl}\ \bar{C} = \sum_I \bar{J}_i\, \delta(\vec{x}-\vec{l}_i)$$

where $\vec{l}_i$ are the odd loops, sources of gauge field $\bar{C}$. Consequently, the energy E of the loops takes the Ampere form.

$$E \approx \varepsilon \sum_{ij} \iint \frac{d\vec{l}_i\, d\vec{l}_j}{|\vec{l}_i-\vec{l}_j|} + \sum_i e_{\mathrm{core}\ i} = \varepsilon \sum_{j=1}^{K} \ln(r_j/a) + K e_{\mathrm{core}}$$

$$E = F\left[-A\rho_f \ln \rho_f + B\rho_f\right] \qquad (4.3)$$

for all, semi-dilute loop geometries[57]. Here, it is convenient to refer sums or integrals to an underlying random network of edge length a, with F faces, L odd loops making up a total of K segments of length a (or threading through K odd faces), core energy e_{core}, so that $\rho_f = K/F =$

$= (a/\zeta)^2$. r_j is the distance from segment j to the nearest, non-adjacent one. In eq. (4.3), the parameters take the values

$$A = \frac{1}{2}\,\varepsilon\, l^3\,, \quad B = e_{core} + \varepsilon \langle \ln (r_j/\zeta) \rangle$$

The leading term in (4.3) is proportional to the only energy scale 6, and only B depends (weakly) on the microscopic structure of the glass through the core structure. This is, of course, the result of the semi-dilute distribution of free odd loops: A semi-dilute distribution has been assumed twice in the derivation of the energy (4.3). First in the linearization of the field theory (2.5-3.3), and second in the evaluation of the Ampere integral (4.3). When the distribution of free odd lines becomes dilute (when T approaches T_0 as we shall see in section 4.5), the logarithmic contribution in (4.3) vanishes, and the energy of each loop adds up, E = B'p$_f$ (dilute).

Elasticity theory yields the same result (4.3) [40,80,57]. Outside the cores of odd lines, the strains and connections are small and the theory can be linearized. Dislocations (which are not topologically stable) screen the strain energy of disclination down to the Ampere form. They also enable disclinations to move, as discussed in section 1.5.

4.3- Entropy of an assembly of free odd loops

The calculation of the previous section, despite starting from a free energy density, kept the odd lines frozen in order to calculate their energy. The entropy of free odd lines, which can move, expand or shrink, cannot be evaluated by the same method, but must be calculated directly.

Let us calculate the number of configurations R of K odd faces (in an underlying random network with a total of F faces), making up an arbitrary number L of distinguishable closed loops. The first loop threads through n_1 odd faces, the second through n_2, etc. L_m is the maximum possible number of loop, n_0 the minimum nurnber ofodd faces threaded through by a single loop, thus X = $L_m/K = 1/n_0 = O(1)$. Let $C(n)/n$ be the number of configurations of a single n-step loop with arbitrary starting point. Typically,

$$C(n)/n \approx (z-1)^n n^{-\beta}$$

with $\beta = 3$ in 3D, but actual numbers are of little relevance to the final result for the entropy (4.4). The number of configurations is given by

$$\Omega = \sum_{L=1}^{L_m} \binom{F}{L} \sum_{n_1 \ldots n_L} \frac{C(n_1)}{n_1} \cdots \frac{C(n_L)}{n_L} \delta(\Sigma n_i - K)$$

The binomial factor is responsible for the entropy of mixing between loops, and $C(n)/n$, for the configurational entropy. In mixtures of loops of arbitrary length, the entropy of mixing of the smaller loops ($\approx \ln K! \approx K \ln K$) is expected to dominate the configurational entropy $\approx K \ln(z-1)$.

One introduces the generating function

$$x^{n_0} g(x) = \sum_{n=n_0} \frac{C(n)}{n} x^n$$

in terms of which Ω is expressed as

$$\Omega = \sum_{L=1}^{L_m} \binom{F}{L} \frac{1}{(K-n_0 L)!} \left[\left(\frac{\partial}{\partial x} \right)^{K-n_0 L} g^L(x) \right]_{x=0}$$

Whenever $1 << L_m << F$, the most probable distribution has overwhelmingly more configurations than all the others, as is well-known in statistical mechanics, thus,

$$\ln \sum_{L=1}^{L_m} \binom{F}{L} \approx \ln \binom{F}{L_m}$$

since $L_m << (1/2)F$, and the entropy is obtained in terms of $\rho_f = K/F$,

$$S = k_B \ln\Omega = k_B F(-X\rho_f \ln\rho_f + Y\rho_f) + O(\ln K) \qquad (4.4)$$

It is dominated, as anticipated, by the binomial coefficient ie. by the entropy of mixing ($X = L_m/K$). The second term in (4.4), $Y = Y_1 + Y_2$, has both mixing ($Y_1 = X - X\ln X$) and configurational ($Y_2 = \ln(z-1) - X\ln(n_0^{\beta})$) origins.

4.4 - Density of free odd lines in thermodynamic equilibrium

Although glass is not strictly in thermodynamics equilibrium,

and the observed "glass transition" is essentially kinetic in character (the fluid-solid crossover is smooth, and occurs at a temperature above T_0 which depends on the cooling rate and on the thermal history of the sample), the time scale for topological modification and for change in the physical properties is much longer than that relevant to the propagation of elementary excitations (eg. phonons) about a metastable state. Thus, slow modes (the density of free odd lines) can be obtained from a thermodynamics derivation, and describe the physical behaviour of the system, even if its linear response is so sluggish as to beinaccessible experimentally very close to T_0.

Thedensity of freeodd linesat a temperature T, $\rho_f(T)$, is that minimizing the free energy F = E - TS, with $E(\rho_f)$ and $S(\rho_f)$ given by eq. (4.3) and (4.4), respectively. One obtains,

$$\rho_f(T) = b\, e^{-c/(T-T_0)} \tag{4.5}$$

which has the Vogel-Fulcher form (1.1) because both energy and entropy have the same functional dependance, $\rho_f \ln \rho_f$. Here $k_B T_0$ = A/X = E is the only energy scale of the problem, as expected (section 3.4). $b = \exp(Y/X) - 1$ and $k_B c = (B - AY/X)/X$ is a positive number because $e_{core} > E$, $(B > A)$.

The density of free odd lines vanishes at T_0, where all odd lines have been frozen by their mutual interaction. Similarly, their entropy also vanishes exponentially at T_0 (Kauzmann paradox),

$$S_f = k_B F\, Xb \left(1 + \frac{c}{T-T_0}\right) e^{-c/(T-T_0)}$$

Below T_0, the odd lines are frozen, and their entropy (which could then be calculated from the free energy density $f(\vec{x})$ (3.3)) is not accessible thermodynamically (eg. from the specific heat). This condensation of odd lines at T_0 is a genuine phase transition, the extrapolation to zero cooling rate of the kinematic "glass transition". However, the assumption of a semi-dilute distribution of odd loops, responsible for the $\rho_f \ln \rho_f$ dependance of the energy (4.3), is not valid close to T_0, and the $\rho_f(T)$ crosses over from Fulcher to Arrhenius behaviour, as we shall discuss in section 4.5.

The viscosity, or any structural relaxation time, then follows the Vogel-Fulcher law (1.1), since its inverse, fluidity, is due to the

diffusion of some topoiogically stable, universal "defect" in glass[78,12,1], here, the odd lines. By dimensional analysis, the length of free odd line per unit volume is $\rho_f a^{-2}$, the average distance between any site in the glass and the nearest odd line is $\rho_f^{-1/2} a$, and the average time $\bar{\tau}$ for the odd line to difuse to that site in order to relax it, is proportional to $\rho_f^{-1} a^2$, so that the fluidity is itself proportional to the density of free odd lines in thermal equilibrium

$$\eta^{-1} \propto \bar{\tau}^{-1} \propto \rho_f(T)$$

4.5 - Crossover to Arrhenius

The Vogel-Fulcher condensation of free odd lines is only a mean field result, valid as long as the distribution of free odd lines remains semi-dilute (cf. derivation of the energy (4.3)). This is not valid close to T_0, where ρ_f is very small. How close will be discussed in this section.

The semi-dilute regime corresponds to

$$\zeta < l \ , \ \rho_f = (a/\zeta)^2 > (a/l)^2 \ , \ T > T_*$$

where the crossover temperature T_* is given by

$$\zeta_0 = [\rho_f(T_0)]^{-1/2} a = l$$

and eq. (4.5). In this regime, the free energy can be linearized, one has a similar situation to electrodynamics of currents loops, and $E \propto \rho_f \ln \rho_f$.

However. when

$$T_0 < T < T_* \ , \ \rho_f < (a/l)^2 \ , \ \zeta > l$$

the distribution of odd lines is dilute, the energy is the sum of individual loop contributions E a ρ_f, A, ie. the "T_0" in eq. (4.5) vanish, and the density of free odd lines crosses over to Arrhenius behaviour. ρ_f is thenlarger than it would have been in the semi-dilute regime at the same temperature (4.5), and the viscosity accordingly falls below the Vogel-Fulcher curve.

Whether the crossver to Arrhenius is observable in a given glass, dependson thenon-collinearity length $l = 1/(\sqrt{\gamma}\lambda_0 g)$. If l is

large, $T_* \simeq T_0$, and $\eta(T_*)$ is large, the crossover is not observable in an experiment lasting a finite time. On the other hand, the crossover is observable if ζ is small. The status of several glasses is reviewed in Cohen and Grest[9].

Although the behaviour of a glass above T_0 can be described by the motion of odd lines, which show a tendency to freeze in a Vogel-Fulcher fashion, the existence of a thermodynamic phase transition is offset by crossover to dilute distribution of odd lines, and to non-linear elastic behaviour. Even within the semi-dilute regime (4.3), the precise nature of the condensation (its universality class) is not known, and cannot be obtained from our rough mean field calculation.

For completeness, and without discussion, let me mention different approaches to the glass transition:

i) All kinematics (no transition).

ii) Statistical mechanics of long polymer molecules[82]. This approximate calculation leads to a phase transition of a very particular type (the continuous relation between energy and entropy cannot persist below a finite temperature), but a counter-example for networks of coordination 2^D has been given by Gujrati and Goldstein[83].

iii) Free volume + percolation theory[72,9].

iv) Floppy (underconstrained) and rigid (overconstrained) regions (first discussed by J.C.Phillips[46]) + percolation theory[84].

The experimental situation is reviewed in ref. [85].

The present approach is by far the most economical, both in the number of parameters and of specific ingredients. We have shown in this paper that the combination of odd lines (as essential structural constituents), and gauge invariance (describing the non generative homogeneity of glass) can explain and control directly and specifically the universal properties of glasses and supercooled liquids.

V – STATISTICAL CRYSTALLOGRAPHY

5.1 - And now for something completely different

In this part, I shall return to the structure, not only of glasses, but of random, space-filling, cellular structures in general, which will be referred to as random tissues, froths, or mosaics in the

case of a 2D pattern. Glasses are represented in this class of structures by the Voronoi froths of amorphous packings and metallic glasses. But such structures abound in nature and in involuntary art (Fig. 10). In 3D, metallurgical aggregates, foams, soap bubble froths, undifferentiated biological tissues, lead-shot packings (Bernal model for the structure of a liquid); in 2D, geological jointings (cracked lava flows like the Giant's Causeway), mud cracking (Pl.2), photographic emulsions, etc., all are random froths.

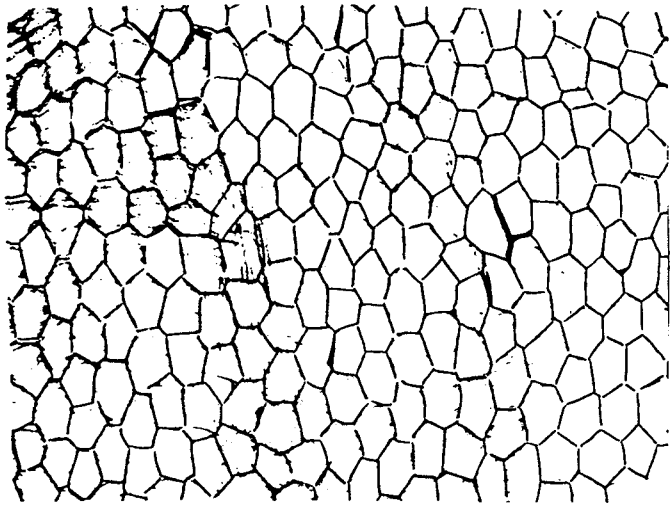

Fig.10 - Window design of an archaic, but common variety in England. "The Bell", Narborough, Leics.: Gentlemen lavatory, left window.

To a first approximation, all these structures are indistinguishible, apart from an obvious scaling factor. This structural similarity is exhibited dramatically in Fig. 1 of Dormer's book[87], in Figs. 2-7 of Weaire's essay[88], and in a recent review of 2D random patterns[17]. One notices also (as befits random structures - section 1.3) a considerable variety of cell shapes. It is improbable that specific physical, or biological forces should be responsible for such identical but variegated architectural style, so that one looks again for universality: An ideal random space-filling structure, determined solely by inescapable, mathematical constraints and the fact that the structure is the

most probable one. It is in statistical equilibrium, in that any topological rearrangement of the cells leaves its "arbitrariness" invariant, the arbitrariness being measured precisely by the entropy or information contained in the structure. One sees immediately the analogy of this programme with statistical mechanics, and with the Maximum Entropy formalism of probability theory[Sg,90]. If such an ideal structure exists, it is the (most probable) representative of an ensemble of structures. It is not unique. Accordingly, criteria for ideality will be relations between averaged, measurable properties of the structure, like the ideal gas law in thermodynamics, rather than geometrical data like unit cells or Bragg spots. One is looking for the statistical analogue of the simple cubic structure in crystallography, or of the ideal gas law in thermodynamics, from which departures can be measured to identify the forces which may differentiate between structures at a second order of approximation.

A few words of apology: To the addict, random patterns are a cause of many delightfully wasted hours. By others, it is regarded as an amusing, and rather trivial hobby, harmless, but without artistic pretensions or cosmic significance. In this respect, it suffers from its very universality: a subject which spans beer froth, crazy paving, cucumber skin and ideal partition of Ireland many not be immediately associated with deep mathematics or ethereal beauty. It is rather vulgar (Fig.10). It is also littered with empty experiments (eg. measuring Euler's theorem, as quoted in ref. [87]), false statements repeated blindly over centuries (eg. that in 3D, cells are 12 -, or, later on, 14-sided on average[19,17]), and irreducible positions stated in dramatic language: Contrast "There are aspects of tissue geometry so obvious that they can hardly escape the attention of any person who seriously considers the question at all. The appreciation that cells are polyhedral figures came with the very first histological report ever published" (ref. 87, p.7-8), with a referee's report from Nature"... the paper, which deals with cells as if they were polyhedra, which they are not...". Incidentally, Dormer is right, but the paper was rejected. The subject started (in the 17th century) as useless, because[19] thestandard activity at the time consisted in packing cannon balls, and random packing of these is unlikely to make one the Ruler of the Queen's Navy, but (in the 1940's), botanists have taken the trouble to compare plant

tissues with the structures of soap bubbles froths, and lead-shot packings, in order to find out which physical force (surface tension or hard-sphere repulsion) was responsible for the structure of biological tissues. Without success as all three types of structures are roughly identical[19].]

There are also several beautiful examples of man-made and natural foams in ref. [104]. M.F. Ashby's conclusions (on the mechanical properties of cellular solids) are very similar to those of this paper: Importance of the structure in determining the mechanical properties of cellular solids, which are roughly independant of the chemical or physical properties of their constituting materials, and universality of the structures, which are well described by a few parameters: cell anisotropy, open or closed cells, and relative density.

5.2 - The random tissue or froth

Random frothlabels the class of structures with whichwe shall be concerned. It is a maximally random, space-filling, cellular structure. Maximal randomness (or "random avoindance of the niceties of adjustment"[21]) means that all vertices, edges and faces are structurally stable (their connectivity is unchanged under a small deformation), i.e., in 3D, 4 edges, 6 faces and 4 cells meeting at every vertex, every edge shared by 3 faces and cells, besides the general property that every face separates 2 cells. In 2D, vertices have 3 incident edges and faces, besides every edge separating 2 faces. Exceptional vertices with more than 4 edges are not structurally stable in 3D: They can be split into 2 normal vertices by infinitesimal transformation (half of T1 of Fig.2). Probability of their occurrence in a random packing is negligibla. The same holds for exceptional edges with more than 3 faces. CRN are excluded from this restricted class of random structures, because their edges may share more than 3 (non-planar) faces, even if their vertices still have 4 edges (albeit for chemical rather than topological reason). Consequently, the 3D relation (eq. (5.2) below) between average numbers of faces per cell and of edges per face, should be modified for CRN. Indeed, it has already been remarked that $\langle n \rangle \approx 7$ in CRN[22].

The structural stability of random froths was discussed in part I, with Voronoi froth as paradigm. They exhibit all the vocabulary

(dislocations, disclinations) and the grammar (elementary transformations) of section 1.5.

There are two topological random variables for the 3D froth, the number f of faces per cell, and the number n of edges per face. For the 2D froth, n is the only topological random variable. They are not independant: Euler's relation (1.2), and the valence relations between incident edges and vertices, etc., discussed above, yield immediately the following topological identities for the random froth

$$\langle n \rangle = 6 \quad (2D) \tag{5.1}$$

$$\langle f \rangle = \frac{12}{6 - \langle n \rangle} \quad (3D) \tag{5.2}$$

which relate the expectation values of the topological random variables. Eq. (5.2) is an identity, which holds *both* for any individual cell in the froth, and for the froth as a whole. Indeed, there are two statistical problems in 3D, one at the froth level, described by the random variable f, and the other at the cell level, where n can still fluctuate (with $\langle n \rangle_{cell}$ determinedbyeq. (5.2)). The two problems are related by (5.2). All this is summarized in the considerable variety ofcell shapes observed[19].

Equations (5.1) and (5.2) are the only *topological* constraints on the statistical structure of the froth.

In 2D, the expectation value of the topological randorn variable $\langle n \rangle$, is fixed by eq. (5.1). In 3D, it is found empirically that most random froths have $\langle f \rangle \approx 14$, but it is, emphatically, *not* an exact result, or even a limit, despite repeated statements in the literature to the countrary (cf. refs. [19] and [17]). A random froth with isotropic cells of equal volumes has $\langle f \rangle = 13.40$, corresponding to the impossible feat (in Euclidean space) of packing 5.1 equal, regular tetrahedra in thedual graph (cf. section 1.3). Fluctuations in thevolumes of the cells reduce $\langle f \rangle$, whereas fluctuations in the angles (anisotropy of the cells) increase $\langle f \rangle$[18], as observed[19,40,91,92,93]. (The high values of $\langle f \rangle$ observed for lead-shot packings[92], are probably due to uniaxial compression causing cell anisotropy, as D.E.G.Williams has aptly remarked). For a Voronoi froth with centres at random (Poisson distribution), Meijering[91] obtains $\langle f \rangle_p = 15.54$ exactly. The cells appear

indeed highly anisotropic.

We now turn to the *correlation* between cell shapes (ie. between the topological variables in neighbouring cells). One knows from experience that large cells tend to have small neighbours, and vice versa. The precise formulation of this result is due to Aboav (empirically)[94], and was made plausible by Weaire[95].

5.3 - Topological correlations, Aboav-Weaire law and microreversibility

In this section, we shall investigate shape correlation between neighbouring cells of the random froth. We shall use a derivation of Aboav-Weaire's relation due to Blanc and Mocellin[96], mainly because it investigates the random froth under the elementary structural transformations of section 1.5. In other, fashionable words, it follows the froth under structural renormalization. As a bonus, we shall obtain the same recursion relation (5.3) for shape correlation under all elementary transformations, T1, T2, mitosis and their inverses. This implies, first, *microreversibility*: all these transforrnations can occur independently of each other in space or time, without affecting the statistical equilibrium of the structure. Second, *statistical equilibirum* itself: a random froth is already very close to, or at a fixed point under structural transformations, with both expectation value (in 20, through (5.1)) and correlation of its topological variable invariant under these transformations.

Let us start with the froth in 2D. The random variable is n, its expectation value is fixed by eq. (5.1), and the topological correlations are given by $m(n)$, the average shape (number of sides) of the nearest neighbours of a n-sided cell. For short, label each cell by the number of its sides. Consider transformation T2 first (Fig. 3): triangular cell d, neighbour to cell a, disappears. Among cell a's neighbours, cells b and c lose one side in the process (as does cell a). The other cells (s) remains unaffected. Thus

$$a\ m(a) = b+c+d+s \xrightarrow[T2]{} (a-1)\ m(a-1) = (b-1) + (c-1) + s$$

Since $d = 3$, one has the recursion relation,

$$a\ m(a) = (a-1)\ m(a-1) + 5 \qquad (5.3)$$

Similarly, for a T1 transformation (Fig. 2) : $a \to a' = a-1$, $b'=b-1$, $c'=c+1$, $d'=d+1$, $s'=s$, hence,

$$a\, m(a) = (a-1)\, m(a-1) + \langle b' \rangle - 1$$

But cell b' is no longer nearest neighbour to a (whereas b was, prior to the transformation), so that, assuming no correlation beyond nearest neighbours, we have $\langle b' \rangle = 6$ (eq.5.1) , and obtain the same recursion relation (5.3) under T1 as under T2. Under the same assumption, one obtainsthe r'th iterate of (5.3) under mitosis where cell a splits into cells r and $a-r+4$,

$$a\, m(a) = r\, m(r) + 5(a-r)$$

Since the same recursion relation holds under T1, T2, mitosis and their inverses, all these transformations can occur independently in space and time (microreversibility), without affecting statistical equilibrium.

The recursion relation (5.3) is readily solved:

$$m(n) = 5 + \frac{B}{n} \tag{5.4}$$

which is the Aboav[94]-Weaire[95] law. It is well obeyed experimentally[17]. (It was originally a purely empirical relation[94], like the other equation of (the statistical equilibrium) state, Lewis's law discussed in the next section). A sum rule due to Weaire,

$$\langle n\, m(n) \rangle = \langle n^2 \rangle = \mu_2 + \langle n \rangle^2 \tag{5.5}$$

relates the parameter B to the variance μ_2 of the distribution of $\{n\}$.

In 3D, there are now two random variables n and f, and there is no relation involving only f and the average number of faces of cells neighbouring cell f, as far as I am aware. However, one obtains the same results as in 2D (Aboav relation, unique recursion relation, and microrecersibility) if one considers what happens to a n-sided face of a f--faceted cell, and its neighbours under structural transformations T1, T2 and mitosis[97], ie. the statistical description of the froth at the cell level. Consider a given, f-faceted cell. Denote as before, by $m_f(n)$, the average number of sides of the neighbouring faces to face n on f. Transformation T1 conserves f, but T2 reduces it: $f'=f-1$ (T2). Also,

there is now a correlation between a^r and b^r_f, despite the fact that they are no longer nearest neighbours (cf. T1), because they belong to the same, finite cell where eq. (5.2) must hold.

When the dust settles, one obtain the 3D Aboav relation[97]

$$n\, m_f(n) = 5f - 11 - C(f-1-n) \qquad (5.6)$$

where C is a parameter of the froth, independant of f. There has been, so far, no experimental verification of eq. (5.6). Weaire's sum rule (5.5) (for a given cell) and eq. (5.2), inserted into (5.6), yield an interesting relation between the variance of the distribution of sides on a f-sided cell, $\mu_{2,f} = \langle [n - \langle n \rangle_f]^2 \rangle_f$, and f

$$\mu_{2,f} = \frac{(f-4)(f-3)}{f}\left[5 - C - \frac{12}{f}\right] \qquad (5.7)$$

Calculating bounds for $\mu_{2,f}$ for small cells ($f = 4, 5$), one obtains $-1 \leqslant C \leqslant 2$.

5.4 - Ideal random froth, most probable distribution and Lewis's law

Let us define statistical equilibrium and universality of random structures.

We begin with the remark that all random, space-filling structures enumerated in section 5.1 are, roughly, identical. They are therefore unlikely to depend on the particular physical, biological or chemical properties of their constituting materials, except for their single length scales. Indeed, the very fact that *random* structures occur (at least in 2D where there is no conflict (frustration) between local packing and global ordering), suggests that specific, short-ranged, directional forces are less important in framing the structure than the inescapable, mathematical and universal constraints (5.1-2, 5.8-9), pertaining to the space which the cells are filling. (Short-ranged forces in 2D give rise to triangular packings or honeycombs, possibly with a few dislocations).

The miracle is that these two mathematical constraints are sufficient to frame in a *precise, observable* fashion the structures generated under their sole or overriding influence. This is clue to randomness and to the fact, well-known in statistical thermodynamics,

that the most probable distribution of cells is overwhelmingly more probable than any other (cf. comments preceding eq. (4.4)).

The complete statistical problem involves two random variables (in 2D), the number n of sides per cell - the topological variable, and the area A of a cell - the metric variable. To obtain an equation of state, it is sufficient to concentrate on the topological variable n only. A full calculation of the most probable distribution $p(n,A)$ will be published elsewhere[97]. Correlation between shapes of neighbouring cells, discussed in the last section, is an automatic consequence of statistical equilibrium, and not an additional constraint.

One looks for the most probable distribution, $\{p_n\}$, of shapes of the cells in the structure, where p_n is the probability of finding a n-sided cell.

$$\left[p_n = \int dA\, p(n,A) \;,\quad \bar{A}_n = \int dA\, p(n,A) A \right]$$

It is that distribution which maximizes the entropy or information[89]

$$S = -\Sigma\, p_n \ln p_n \tag{5.7}$$

subject to constraints corresponding to our prior knowledge of the system. For *all* random space-filling structures, the constraints are

$$\Sigma\, p_n = 1 \quad \text{(normalization)}$$

$$\Sigma\, p_n \bar{A}_n = A_0/F \quad \text{(space-filling)} \tag{5.8}$$

$$\Sigma\, p_n\, n = 6 \quad \text{(topology)} \tag{5.1}$$

in 2D. In 3D, (5.8) and (5.1) are replaced by

$$C\, p_f\, \bar{V}_f = V_0/C \quad \text{(3D space-filling)} \tag{5.9}$$

$$\Sigma\, p_f\, f = \frac{12}{6-\langle n \rangle} \quad \text{(3D topology)} \tag{5.2}$$

respectively. Here $\bar{A}_n$ is the average area of a n-sided cell, and A_0 the total area available to the F cells in the 2D mosaic. Similarly, *mutatis mutandis*, in 3D. This is all. The problem, as formulated, is entirely mathematical. The constraints are also all mathematical. Physics

(or biology, ...) is absent at this level, so that the resulting structures are universal. The only subjective step is in the coding of the structure by the sole, topological parameter n, and the requirement that it is in statistical equilibrium.

We do not need to evaluate the entropy, or the most pi-obable distribution $\{p_n\}$; the "equation of state" can be obtained by the following argument of Lissowski and myself[27] (fully confirmed by a full calculation[97,57]). The constraints are a linear systems of equations between p_n, so that the smaller the dimensionality of the space of constraints (≤ 3), the larger that of the space of possible solutions $\vec{p} = (p_3, p_4, p_5, \ldots)$, and the more probable one such solution will be. The most probable distribution is obtained by reducing as much as possible the dimensionality of the space of constraints, by making them linearly dependant,

$$\bar{A}_n = (A_0/F)\,\lambda\,[n - (6 - 1/\lambda)] = (A_0/F)\,[\lambda\,(n-6) + 1] \qquad (5.10)$$

The averaged area of a n-sided cell, $\bar{A}_n$, is linearly related to the number n of its sides. [The intercept $n_0 = (6 - 1/\lambda)$]. This relation was suggested empirically in 1928 by Lewis[27], on the basis of observations on cucumber epidermis, human amnion and the pigmented epithelium of the retina. Most undifferentiated biological tissues obey it[99]. It is also obeyed by Voronoi froth generated from Poisson-distributed centres[98], albeit with a smaller intercept ($n_0 \simeq 0$ instead of $\simeq$ 1-2 in biological mosaics), but not, usually, by metallurgical grain agregates, as will be discussed below. It is a relation between averaged, observable parameters of the random froth, ie. the equation of state of statistical crystallography describing an ideal froth (in the same sense as "ideal gas" in thermodynamics).

The effective elimination of one constraint, leading to Lewis's law (5.10), increases the entropy further. This is because, as in statistical thermodynamics, the most probable entropy $S(X_i)$ (5.7) is a convex function of its variables, the right-hand sides of the constraint equations (5.1) and (5.8), written generally $\sum p_n c_{ni} = X_i$, and imposed by Lagrange multipliers λ_i[89]

$$S(X_i) = \ln \{ \sum_n e^{\left(\sum_i \lambda_i c_{ni}\right)} \} - \sum_i \lambda_i X_i$$

$$\frac{\partial^2 S}{\partial X_i^2} \leq 0$$

(specific heats are positive). Let $i=s$ be the constraint we wish to eliminate, imposed by Lagrange multiplier λ_s. As a function of X_s, S is maximum when $\partial S/\partial X_s = 0$. But $\partial S/\partial X_s = -\lambda_s$, and $A_s = 0$ states precisely that constraint s is no longer operative, in our case because it is no longer independant of the others[S7].

This derivative of Lewis's law goes therefore one step beyond the standard applications of the Maximum Entropy formalism[89,90], in which the functional form of the constraints is known a *priori*. Here, we have taken advantage of the liberty to *adjust* the functional form of the constraints in order to maximize *further* the entropy.

There exists, at least in principle, an alternative to Lewis's law in decreasing the dimensionality of constraint space: It relates linearly the space-filling constraint to the normalization, instead of the topology constraint, and yields $\bar{A}_n$ = cst, independant of n, that is no correlation between cell shapes and sizes. Even though this solution also maximizes further the entropy, it does not occur in natural froths or mosaics, but for no mathematical reason as far as I known. This remark shows that further increase of the entropy corresponds to a choice between *discrete* alternatives.

The parameter λ in (5.10) is the undetermined Lagrange multiplier imposing the linearly dependant constraints (S. I) and (5.8). (The other multiplier is eliminated because of the linear dependance of the constraints). It is related to the slope and intercept of Lewis's relation, and is therefore an important descriptive parameter of the structure. Moreover, Lagrange multipliers have a habit in thermodynamics and in mechanics of possessing a physical meaning of their own. They are not merely arbitrary mathematical factors. What is, therefore, the measning of λ ? We shall see in next section that it measures the ageing of the structure.

Lewis's law is *not* obeyed by 2D metallurgical grain aggregates, whether experimentally, or in computer simulations by the EXXON group[100], where it is the grain's radius (or its perimeter) $\bar{R}_n$, which is proportional to n, rather than its area as in Lewis's law. According to the methodology of Maximum Entropy formalism, this fact demonstrates

the existence of new constraint, besides the mathematical ones. Clearly, in the computer simulations of grain growth and statistics by the EXXON group, and as demonstrated experimentally[101], it is the *energy* associated with grain boundary length which is the driving mechanism for grain growth and statistical equilibrium. [The EXXON group model grain statistics and dynamics by a ($\{l\}$=64 $\approx$ ∞-state) ferromagnetic Potts model (a generalization of the Ising model to more than 2 states), on which they carry Monte-Carlo simulations. Every grain is characterized by a different orientation of the Potts spin, ie. by a different value of l. All the energy is carried by the interfaces, where the "spins" are not "parallel", so that the energy is proportional to the perimeter (ie. $\bar{R}_n$) of the cell]. The additional, physical constraint is simply the energy

$$\Sigma\, p_n \bar{R}_n = E \,. \tag{5.11}$$

This provides an alternative to Lewis's law in reducing by 1 the dimensionality of the constraint space, namely[97]

$$\bar{R}_n = \alpha (n - n_0') \tag{5.12}$$

as observed experimentally and in the simulation. One can show that at $T \approx 0$ (ie. with the Lagrange multiplier imposing the energy constraint (5.11) $\approx \infty$), the maximal entropy using alternative (5.12) is larger than using Lewis's alternative (5.10)[97]. This example emphasizes the *diagnostic* power of the Maximum Entropy formalism. A relevant physical constraint has been uncovered by noticing the discrepancy between observed and ideal equations of state.

The most drastic reduction (by 2) of the dimensionality of constraint space, and the largest entropy, would occur in a polycrystalline aggregate where all constraints are linearly dependant, ie. $\bar{R}_n - \bar{A}_n - n$, or its equivalent in 3D. Such scaling between perimeter and area of cells is clearly impossible in 2D, but would be possible in principle in 3D, if the cell boundaries were fractal (dendritic). But then, reduction in the energy would no longer be the driving force for grain growth and statistical equilibrium.

It is elementary to generalize Lewis's law to 3D random froths[18]

$$\bar{V}_f = (V_0/C)\,\lambda\left[f - (\langle f\rangle - 1/\lambda)\right] \qquad (5.13)$$

but this relation has not yet been confirmed experimentally.

5.5 - Evolution of a random froth. Von Neumann's law

Many random cellular structures evolve (slowly) in time. In soap bubble froths, gas diffuses across the interface between bubbles. Biological tissues undergo growth and cell divisions. In metallurgical aggregates, large grains grow at the expense of small ones, in a controlled process called sintering, etc. The time scale for this evolution is much longer than that associated with mechanical response of the structure, so that it can be assumed that the random froth, once in statistical equilibrium, remains in statistical equilibrium at all times. Consequently, Lewis's law (5.10-13) is expected to holdthroughout the evolution of the structure. The parameters A_0, F, and speciallythe hitherto undetermined Lagrange multiplier h, have their own, specific evolution.

The simplest case is the evolution of a 2D froth with constant total area A_0 and constant number of cells F. It refers to time intervals not long enough for bubbles to disappear (no T2 process) in a soap bubble froth, or for a cell to divide in a biological tissue. Differentiating Lewis's law with respect to time, one obtains the rate of growth of an averaged n-sided cell,

$$\frac{d\bar{A}_n}{dt} = \frac{A_0}{F}\frac{d\lambda}{dt}(n-6) = \gamma(n-6) \qquad (5.14)$$

This result was actually derived by von Neumann[102], for 2D soap bubble froths exclusively. (Actually, von Neumann's result for soap bubbles is slightly stronger than eq. (5.14), as it involves the rate of growth of every individual bubble rather than its average for all n-sided cells as in (5.14)). Von Neumann's derivation relied on the *physical* mechanism of evolution of a soap bubble froth and on three assumptions specificto this particular system, even though the final result (5.14) is topological: A pentagonal cell loses area at the same rate as a heptagonal cell gains it, and at half the rate of an octogonal cell, etc., regardless of their geometrical shapes or areas. Our derivations[103] is com-

pletely general and topological, so that von Neumann's law (5.14) is applicable to any evolving mosaic, and generalizable to 3D random froths, since Lewis's law, and statistical equilibrium, can also be generalized to 3D.

[Von Neurnann's derivation of (5.14) required a) a specific physical mechanism for the evolution of a soap bubble froth: dif'fusion of the (incompressible) gas across the interface between two bubbles, at a rate proportional to the pressure difference between the bubbles, ie. to the radius of curvature of their interface, and b) three, crucial assumptions: i) incompressible gas, ii) interfaces meeting at 120^{o} on vertices, and iii) 2D system. Yet, the result is topological.]

For a soap bubble froth, $(A_0/F)\chi = y = (2\pi/3)\delta\sigma > 0$, where a is the surface tension of the interfacial liquid, and δ, itç diffusivity[102]. γ is therefore a constant of the froth, invariant in time, at least as long as the interfacial liquid does not change appreciably in thickness. This provides the physical interpretation of the Lagrange multiplier λ:

$$\lambda = \gamma (F/A_0)\, t + \lambda_0$$

λ measures therefore the *ageing* of the structure (or, simply, the time). This is so even if F, A and y evolve with time (mitosis, T2 process, etc.),

$$\lambda = (F/A_0) \int \gamma \, dt \qquad (5.15)$$

but then, the cells which do not evolve in time are no longer hexagonal as in (5.14), but n_1-sided, with n_1 given by

$$n_1 = 6 - \frac{1}{\gamma} \frac{d(A_0/F)}{dt}$$

Computer-generated Voronoi froths with Poisson centres[98] are "as-quenched", younger structures ($\lambda = 1/6$, Lewis intercept $n_0 = 0$) than biological tissues[27,99], which are "aged" ($\lambda = 1/4$, $n_0 = 2$). Ageing affects also the appearance of the structure, where cells become more isotropic and differentiated in sizes as time, ie. χ or n_0 increases.

As Lewis's law, and statistical equilibrium can be extended to 3D froths, von Neumann's law can also be generalized to 3D structures[103]. In particular, over short periods when C and $\langle f \rangle$ are ccinstant in time, one has

$$\frac{d\bar{V}_f}{dt} = \delta (f - \langle f \rangle)$$

with $\langle f \rangle$ given by eq. (5.2). The Lagrange multiplier in Lewis's law still measures ageing of the structure.

5.6 - Conclusions

We have seen that statistical crystallography, a method to describe and classify the structure of amorphous materials, can usefully be set up, along the guidelines of established statistical thermodynamics[ag]. It actually goes one step beyond statistical hermodynamics, as one can take advantage of the arbitrariness in the functional dependance of one the constraints to maximize further the entropy. The constraints (ie. the statistical ensemble) are easily selected: They are purely mathematical, pertaining to the topology of the space which the structure is filling. There may be additional constraints, which are then physical or biological. In the absence of these additional, specific constraints, the random structure is called *ideal*, by analogy with ideal gas in thermodynarnics. It equation of state (Lewis's law) is experimentally observable, as is the ideal gas law. Deviations from Lewis's law betray the presence and structural relevance of specific (physical, biological,. ..) forces, which are obviously worth identifying, exactly as departures from the ideal gas law yield information, through the virial expansion, on interatomic forces and, ultimately, on other phases of matter. As in statistical thermodynamics, statistical equilibrium, and Lewis's law, are consequences of the balance between entropy (most probable distribution), and the lowest level of organization (space-filling, territorial partition, encoded by the constraints)

Acknowledgements

Denis Weaire has kindly let me use his cartoon (Fig.1) to illustrate topological equivalence. I am very grateful to him also for all the arguments we have had over the years about many points raised in this paper. Figs.2-6 have been taken from ref. [17], Fig. 7 from ref. [57].

Dorothy Duffy, Andrei Lissowski and Helena Gilchrist have made substantial contributions to the material presented have. Discussions with D. Bovet, A. Comtet, N.R. Da Silva, F. Dowell, J.-M. Dubois, C. Eilbeck, H.L. Frisch, J.P.Gaspard, M. Goldstein, O. J. Greene, H. Guentherodt, J.Jaeckle, R.Kerner, M.Kléman, J. Malbouisson, R.Mosseri, T.Ninomiya, J.F.Sadoc, J. Sethna, J.Spalek, G.Toulouse, M.F. Thorpe and D.E.G. Williarns are gratefully acknowledged.

I am grateful to the CNLS and CMS, Los Alamos National Laboratory, and to the organizers of the Latin-American Symposium on the Physics of Amorphous Systems, Niteroi 1984, for the opportunity to present and prepare the lectures that were at the source of this paper. Financia1 support by the British Council, CNPq, SERC and CNLS-CMS is acknowledged with thanks.

REFERENCES

1. P.W.Anderson, in *III-Condensed Matter,* R. Balian, R.Maynard and G. Toulouse, eds., North Holland (1979), 159.
2. J.L.Black, in *Amorphous Metals I*, H.J.Guentherodt and H.Beck, eds., Springer (1981), 167.
3. G.Toulouse and M.Kléman, J. Physique Lettres, 37, L-149 (1976); G.E. Volovik and V.P.Mineev, Zh.Eksp.Teor.Fiz.Pis'ma, 23, 647 1 9; N. D.Mermin, Rev.Mod.Phys., 51, 591 (1979); L.Michel, Rev. Mod. Phys., *52,* 617 (1980); G.Toulouse, Phys. Rep., 49, 267 (1979). For an excellent introduction, see G.Toulouse, in *Modern Trends in the Theory of Condensed Matter;* A.Pekalski and J.Przystawa, eds., Springer, 189 (1980).
4. N.Rivier, Phil.Mag.A, 40, 859 (1979).
5. W.A.Phillips, *Amorphous Solids. Low-Temperature Properties,* Topics in Current Physics, 24, Springer (1981).
6. P.W.Anderson, B.I.Halperin and C.M.Varma, Phil. Mag., 25, 1 (1972); W.A.Phillips, J.Low Temp. Phys., 7, 351 (1972).
7. B.Golding and J.E.Graebner, in ref. 5, 107 (1981).
8. H.E.Hagy, in *Introduction to Glass Science,* W. C. LaCourse, eds., Plenum 343, (1972).
9. See, for example, D. Turnbull and B.G. Bagley, in *Treatise on Solid State Chemistry,* N. B. Hannay, ed., Plenum 5, 513 (1975). M.H.Cohen

and G.S .Grest, Phys. Rev. B, 20, 1077 (1979).

10. C.A.Angell and K.J.Rao, J.Chem.Phys., 57, 470 (1972); C.A. Angell and J.C.Tucker, J.Phys.Chem., 78, 278 (1974).
11. J.Jaeckle, Phil.Mag.B, 44, 533 (1981); J.Jaeckle, Physica B and C 127, 79 (1984).
12. J.Frenkel, *Kinetic Theory of Liquids*, Dover (1955), ch.IV.2.
13. D.Weaire, Phys.Rev.Letters, 26, 1541 (1971).
14. D.Weaire and M.F.Thorpe, Phys. Rev. B, 4, 2508 (1971). A very readable account is given in the lectures notes: M.F.Thorpe, *Some Aspects of Disordered Solids*, UFF Publ., Niteroi (1980).
15. E.A.Davis, Phil.Mag., 38, 463 (1978).
16. R.Zallen, in *Fluctuation Phenomena*, E. W.Montroll and J.L. Lebowitz, eds., North Holland (1979), ch.3.
17. D.Weaire and N.Rivier, Contemp.Phys., 25, 59 (1984).
18. N.Rivier, J.Physique (Coll.), 43, C9-91 (1982).
19. E. B.Matzke, Am.J.Botany, 33, 59 (1946). See also the "detective story": E.B.Matzke, Bull. Torrey Botan. Club, 27, 222 (1950).
20. B.Gruenbaum and G.C.Shephard, *Tilings and Patterns*, to be published by W.H. Freeman, ch. 10; R.Mosseri and J.F.Sadoc, in *Structure of Non-Crystalline Materials* 1982, P.H. Gaskell, E.A.Davis and J.M.Parker, eds., Taylor and Francis (1983), 137; M.Gardner, Scientific Amer., *236/1*, 110 (1977).
21. F.T.Lewis, Am.J.Botany, 30, 74 (1943).
22. See for example: P.Steinhardt and P.Chaudhary, Phil.Mag.A, 44, 1375 (1981).
23. H.S.M.Coxeter, *Introduction to Geometry*, Wiley (1961), ch. 6.5.
24. B.J.Gellatly and J.L.Finney, J.Non-cryst.Solids, 50, 313 (1982); J. L.Finney, B.J.Gellatly and J.P. Ebuquiere, in *Amorphous Materials: Modeling of Structure and Properties*, V.Vitek, ed., TMS-AIME (1983), 3.
25. *Glass and W.E.S.Turner*, E.J.Gooding and E.Meigh, eds., Soc.of Glass Techn. (1951).
26. F.Bloch, Phys. Rev. B, 2, 109 (1970).
27. F.T. Lewis, Anat. Rec., 38, 341 (1928); N.Rivier and A. Lissowski, J.Phys. A, *15*, L143 (1982).
28. Valence alternation pairs have been suggested by Mott, Street and

Davis and independently by Kastner, Adler and Fritsche. See R.Zallen *The Physics of Amorphous Solids*, Wiley (1983), 105.

29. H.He and M.F.Thorpe, unpublished.
30. D. Weaire and J.P.Kermode, Phil.Mag.B, 48, 245 (1983).
31. F.Wooten and D.Weaire, J.Non-cryst.Solids, 64, 325 (1984); F.Wooten, G.A.Fuller, K.Winer and D.Weaire, J.Non.cryst. Solids, 75, 45 (1985).
32. H.M.Princen, J.Colloid.Interface.Sci., 91, 160 (1983).
33. N.Rivier, R.Occelli, J.Pantaloni and A.Lissowski, J.Physique, 45, 49 (1984).
34. F.T.Lewis, Am.J.Botany, 30, 766 (1943); M.B.Pyshnov, J.Theor.Biol. *87*, 189 (1980).
35. M.Hillert, Acta Met., *13*, 227 (1965).
36. J.E.Morral and M.F.Ashby, Acta Met., 22, 567 (1974).
37. N.Rivier and D.M.Duffy, J.Physique, 43, 293 (1982).
38. J.P.Gaspard, R.Mosseri and J.F.Sadoc, Phil.Mag.B, (1984) to appear.
39. T. Ninomiya, in *Topological Disorder in Condensed Matter*, F.Yonezawa and T.Ninomiya, eds., Springer Series in Solid State Sciences 46, 40 (1983); T.Ninomiya, in *Structure of Non-Crystalline Materials* 1982, ref. [20], 558 (1983).
40. D.M.Duffy and N.Rivier, J.Physique (Coll.), *43*, C9-475 (1982).
41. N.Rivier, J.Physique (Coll.), 39, C6-984 (1978).
42. N.Rivier and D.M.Duffy, J.Phys.C, 15, 2867 (1982).
43. D.Bovet, SM Archives, 4, 31 (1979).
44. M.Kléman and J.F.Sadoc, J.Physique Lettres, *40*, L-569 (1979).
45. J.P.Gaspard, R.Mosseri and J.F.Sadoc, in *Structure of Non-Crystalline Materials* 1982, ref. [20], 550 (1983); D. R.Nelson, P.J.Steirihardt and M.Ronchetti, Phys. Rev. B, 28, 784 (1983); R.Mosseri, Thèse, Univ.de Paris-Sud, Orsay, (1983); J.P.Sethna, Phys.Rev.Letters, 51, 2198 (1983).
46. J.C.Phillips, Solid State Phys., 37, 93 (1982); J.C.Phillips, Phys. Today, 35, 27 (1981).
47. J.F.Sadoc and R.Mosseri, in *Topological Disorder in Condensed Matteq* ref. [39], 30 (1983).
48. J.F.Sadoc, J.Physique Lettres, 44, L-707 (1983). See also D.R.Nelson, Phys. Rev. Letters, 50, 983 (1983).
49. G.Toulouse, Commun.Phys., 2, 115 (1977) and in *Modem Trends in the*

Theory of Condensed Matter, ref. [3], 195 (1980).
50. E.Fradkin, B.A.Huberman and S.H.Shenker, Phys. Rev. B, *18*, 4789 (1978).
51. M.Kac, Ark.Det.Fysiske Sem.Trondheim, 11, 1 (1968); S.F.Edwards and P.W.Anderson, J.Phys. F, 7, 965 (1975). The trick has been used to average a logarithm in G.H.Hardy, J.E. Littlewood and G.Polya, *Inequalities*, Cambridge Univ.Press (1934), 6.8.
52. D.Sherrington and S. Kirkpatrick, Phys.Rev.Letters, 35, 1792 (1975).
53. C.L.Henley, H.Sompolinsky and B.I.Halperin, Phys.Rev.B, 25, 5849 (1982); E.M.Gullikson, D.R.Fredkin and S.Schultz, Phys.Rev.Letters, 50, 537 (1983); A.Fert and F.Hippert, Phys.Rev.Letters, 49, 1508 (1982); H.Sompolinsky, G.Kotliar and A.Zippelius, (1984) to be published.
54. See for exarnple A. Houghton, S.Jain and A.P.Young, J.Phys.C, *16*, L375 (1983).
55. I.E.Dzyaloshinskii and G.E.Volovik, J.Physique, 39, 693 (1978).
56. J.A.Hertz, Phy.Rev.B, *18*, 4875 (1978).
57. N.Rivier, in *Structure* of *Non-Crystalline Materials* 1982, ref. [20], (1983), 517; N.Rivier, in *Amorphous Materials*, ref. [24], (1983), 81.
58. N.Rivier, *in Topological Disorder in Condensed Matter*, ref. 39, (1983), 14.
59. A.Kadic and D.G.B.Edelen, A *Gauge Theory* of *Dislocations* and *Disclinations*, Springer (1983).
60. E.Kroener was the first to exploit gauge invariance in elasticity. See E.Kroener, in *Physics* of Defects, R.Balian, M.Kléman and J.P. Poirier, eds., North Holland (1981), ch.3.
61. A.Comtet, Phys.Rev.D, 18, 3890 (1978).
62. B.Julia and G.Toulouse, J.Physique Lettres, 40, L-395 (1979).
63. V.Poenaru and G.Toulouse, J.Physique, 38, 887 (1977).
64. Natanael.R.DaSilva, PhD Thesis, Imperial College, London University (1980); N.Rivier, in *Theory* of *Magnetic Alloys*, J.Morkowski and S. Klama, eds., IFM-PAN Poznan, (1980), 67.
65. C.N.Yang and R.L.Mills, Phys.Rev., 96, 191 (1954).
66. J.C.Lasjaunias, R.Maynard and M.Vandorpe, J.Physique Coll., 39, C6 -973 (1978).
67. R.O.Pohl, in ref. [5], 27 (1981).
68. U.Bartell, Dr.rer.nat.thesis, Univ. Konstanz (1983); U.Bartell 'and

S.Hunklinger, J.Physique Coll., 12, C9-489 (1982).

69. D.E.Farrell, J.E.de Oliveira and H.M.Rosenberg, in *Phonon Scattering in Condensed Matter,* Springer (1984), 422.
70. M.Tinkham, *Introduction to Superconductivity,* McGraw Hill, (1975).
71. G.A.N.Connell and R.J.Temkin, Phys.Rev. B 9, 5323 (1974). See also the spin glass equivalent D.C.Mattis, Phys. Lett.,*56* A, 421 (1976).
72. M.H. Cohen and G.S. Grest, Ann.NY Acad.Sci., *371*, 199 (1981).
73. A.R.Cooper, J.Physique (Coll.), *43*, C9-369 (1982).
74. T.L.Smith, P.J.Anthony and A.C.Anderson, Phys.Rev.B, *17*, 4997 (1978).
75. R.H.Stolen, J.T.Krause and C.R.Kurkjian, Disc.Faraday Soc., *50*, 103 (1970).
76. N.Rivier, LT-17 Karlsruhe (1984), and to be published.
77. N.Rivier and H. Gilchrist, J.Non-cryst.Solids *75*, 259 (1985).
78. S.H. Glarum, J.Chem.Phys., 33, 639 (1960); M.C.Phillips, A.J. Barlow and A. Lamb, Proc. Roy.Soc., A *329*, 193 (1972).
79. R.Savit, Rev.Mod.Phys. 52, 453 (1980).
80. D.M.Duffy, PhD Thesis, Imperial College, University of Londori (1981).
81. E.T.Jaynes, "The Well-Posed Problem", Foundations of Physics, *3*,477 (1973).
82. J.H. Gibbs and E.A.DiMarzio, J.Chem.Phys., 28, 373 (1958); E.A.Di-Marzio, Ann.NY Acad.Sci., 371, 1 (1981).
83. P.D.Gujrati and M.Goldstein, J.Chem.Phys., 74, 2596 (1981).
84. M.F.Thorpe, J.Non-cryst.Solids, *57*, 355 (1983); 76, 109 (1985).
85. A.E.Owen, Trieste Lectures (1982).
86. N.Rivier and D.M.Duffy, in *Studies in Critica2 Phenomena,* J.Della--Dora, J. Demongeot and B.Lacolle, eds., Springer Series in Synergetics, *9*, 132 (1981).
87. K. J.Dormer, *Fundamental Tissue Geometry for Biologists,* Cambridge UP (1980).
88. D. Weaire, in *Topological Disorder in Condensed Matter,* ref. [39], 51 (1983).
89. E.T.Jaynes, Phys.Rev., 106, 620 (1957); 108, 171 (1957).
90. E.T.Jaynes, in *The Maximum Entropy Formalism,* R.D.Levine arid M. Tribus, eds., MIT Press, (1979), 15.
91. J.L.Meijering, Phillips Res. Rep., 8, 270 (1953).
92. J.W.Marvin, Am.J.Botany, 26, 280 (1939).

93. E.B.Matzke and J.Nestler, Am.J.Botany, 33, 130 (1946).
94. D.A.Aboav, Metallogr., 3, 383 (1970).
95. D.Weaire, Metallogr., 7, 157 (1974).
96. M.Blanc and A.Mocellin, Acta Met., 22, 1231 (1979).
97. N.Rivier, Phil.Mag. B 52, 795 (1985).
98. I.K.Crain, Computers and Geosc., 4, 131 (1978).
99. V.V.Smoljaninov, *Mathematical Models of Tissues*, Nauka, (1980), ch. 3 (in Russian).
100. D.J.Srolovitz, M.P.Anderson, P.S.Sahni and G.S. Grest, Acta Met., 32, 793 (1984); P.S.Sahni, D.J.Srolovitz, G.S.Grest, M.P.Anderson and S. A.Safran, Phys.Rev.B, 28, 2705 (1983).
101. J.E.Burke, Trans.AIME, 180, 73 (1949).
102. J.von Neumann, in *Metal Interfaces*, Amer.Soc.for Metals, (1952), 108.
103. N.Rivier, Phil.Mag.B, 47, L-45 (1983).
104. M. F.Ashby, Metall.Trans.A, 24, 1755 (1983).
105. J.Joffrin, in *III-Condensed Matter*, ref.[1], (1979), 64
106. M.H. Cohen and L.Turkevich, in Anais do Simpósio Latino Americano de Física dos Sistemas Amorfos, Vol.II, ed. by Enrique Anda, UFF and CLAF publ., Niteroi 1984, 265; M.H. Cohen, in Topological Disorder in Condensed Matter, ref. [39], 122 (1983).

Resumo

As propriedades físicas do vidro são consequências diretas de sua estrutura não cristalina. A estrutura é descrita de um ponto de vista topológico, pois a topologia & a única geometria que sobrevive a não cristalinidade, isto é, a ausência de métrica e de grupo espacial trivial. Este fato tem duas consequências principais: a homogeneidade global do vidro é uma simetria de gauge e os únicos constituintes extensos e estruturalmente estáveis são linhas ímpares (ou disclinações de 2π no limite contínuo elástico). Uma teoria de gauge do vidro, baseado em linhas ímpares como fontes de deformações, congeladas pode explicar aquelas propriedades dos vidros que são ambas específicas e universais nos sólidos amorfos: excitações de baixa temperatura e relaxação a altas temperaturas. Os métodos de mecânica estatística podem ser aplicados para dar uma descrição minimal das estruturas amorfas em equilíbrio estatístico. Critérios para equilíbrio estatístico da estrutura e para balanço detalhado são fornecidos, junto com equações de estado estruturais que são bem conhecidas empiricamente na botânica e metalurgia. Esta resenha é baseada em um curso ministrado em 1984 em Niterói. Ela contêm cinco partes: I - Estrutura, de um ponto de vista topológico; II - Invariância de Gauge; III - Modos de tunelamento; IV - Líquidos superesfriados e transição vítrea; V - Cristalografia estatística.